Available online at www.sciencedirect.com
ScienceDirect
Polymer 48 (2007) 6729–6747
polymer
www.elsevier.com/locate/polymer

Feature Article

Preparation of nanoparticles by the self-organization of polymers consisting of hydrophobic and hydrophilic segments: Potential applications

Takami Akagi [a,c], Masanori Baba [b,c], Mitsuru Akashi [a,c,*]

[a] Department of Applied Chemistry, Graduate School of Engineering, Osaka University, 2-1 Yamadaoka, Suita, 565-0871, Japan
[b] Division of Antiviral Chemotherapy, Center for Chronic Viral Diseases, Graduate School of Medical and Dental Sciences, Kagoshima University, 8-35-1 Sakuragaoka, Kagoshima 890-8544, Japan
[c] Core Research for Evolutional Science and Technology (CREST), Japan Science and Technology Agency (JST), Kawaguchi Center Building, 4-1-8 Honcho, Kawaguchi, 332-0012, Japan

Received 28 May 2007; received in revised form 10 August 2007; accepted 17 August 2007
Available online 21 August 2007

Abstract

This review describes the preparation of core-corona type polymeric nanoparticles and their applications in various technological and biomedical fields. Over the past two decades, we have studied the synthesis and clinical applications of core-corona polymeric nanoparticles composed of hydrophobic polystyrene and hydrophilic macromonomers. These nanoparticles were utilized as catalyst carriers, carriers for oral peptide delivery, virus capture agents, and vaccine carriers, and so on. Moreover, based on this research, we attempted to develop novel biodegradable nanoparticles composed of hydrophobic poly(γ-glutamic acid) (γ-PGA) derivatives (γ-hPGA). Various model proteins were efficiently entrapped on/into the nanoparticles under different conditions: encapsulation, covalent immobilization, and physical adsorption. The encapsulation method showed the most promising results for protein loading. It is expected that biodegradable γ-hPGA nanoparticles can encapsulate and immobilize various biomacromolecules. Nanoparticles consisting of hydrophobic and hydrophilic segments have great potential as multifunctional carriers for pharmaceutical and biomedical applications, such as drug, protein, peptide or DNA delivery systems.

Keywords: Nanoparticles; Drug delivery system; Protein carrier

1. Introduction

Nanoparticles prepared from synthetic or natural polymers have applications in various technological and biomedical fields, because their chemical structures, surface functionalities, and particle size can be easily controlled. Nanoparticles can be defined as colloidal systems with a diameter smaller than 1000 nm [1,2]. Several methods have been developed for preparing nanoparticles. These methods can be divided into two broad categories according to whether the formulation requires a polymerization reaction or can be synthesized directly from a systemic prepared or natural polymer [3]. Nanoparticles with entrapped therapeutic agents, such as small molecules, peptides, proteins and DNA, have recently been shown to possess significant potential as drug delivery systems and adjuvants [4–8]. A colloidal delivery system is one of the most promising because it may reduce unwanted toxic side effects and improve the therapeutic effect. These delivery systems include nanoparticles, liposomes, microemulsions, polymeric self-assemblies, and so on.

Recently, self-assembling block copolymers or hydrophobically modified polymers have been extensively investigated in the field of biotechnology and pharmaceuticals. Amphiphilic

* Corresponding author. Department of Applied Chemistry, Graduate School of Engineering, Osaka University, 2-1 Yamadaoka, Suita, 565-0871, Japan. Tel.: +81 6 6879 7356; fax: +81 6 6879 7359.
E-mail address: akashi@chem.eng.osaka-u.ac.jp (M. Akashi).

0032-3861/$ - see front matter © 2007 Elsevier Ltd. All rights reserved.
doi:10.1016/j.polymer.2007.08.038

block or graft copolymers form self-assembled, nano-sized micelle-like aggregates of various morphologies in aqueous solution [9,10]. In general, self-assembled nanoparticles are composed of an inner hydrophobic core and an outer shell of hydrophilic groups. Hydrophobic blocks form the inner core of the structure, which act as a drug incorporation site, especially for hydrophobic drugs. Hydrophobic drugs can thus be easily entrapped within the inner core by hydrophobic interactions. These self-aggregating characteristics of the polymers have attracted considerable attention as effective targetable drug carriers, for example polyion complex micelles [11] and hydrophobized polysaccharides. Among the different carriers for controlled drug delivery, there has been rising interest in nano-sized self-aggregates composed of natural polysaccharides, such as pullulan [12,13], curdlan [14], dextran [15], alginic acid [16] and chitosan [17]. It was reported that self-aggregated hydrogel nanoparticles could be formed from cholesterol-bearing pullulan by an intra- and/or intermolecular association in diluted aqueous solution [18].

Over the past two decades, we have developed a synthetic method for polymeric nanoparticles based on the free radical copolymerization of hydrophilic macromonomers, which are vinylbenzyl group-terminated water-soluble polyvinyl compounds, with hydrophobic monomers (styrene and methyl methacrylate) in polar organic solvents [19]. During polymerization, amphiphilic graft polymers assemble in solution to form core-corona type nanoparticles, which have hydrophobic cores and hydrophilic corona layers on their surfaces, resulting in an excellent aqueous dispersion [20]. Moreover, our group recently developed novel biodegradable nanoparticles composed of hydrophobically modified poly(γ-glutamic acid) (γ-PGA) prepared by the covalent attachment of L-phenylalanine ethylester (L-PAE). This amphiphilic γ-PGA formed monodispersed nanoparticles or nanofibers in water and the nanoparticles did not induce any cytotoxicity [21,22]. We have also reported nanoparticles comprised of poly(ε-lysine) bearing cholesterol [23].

In this review, we summarize the preparation of core-corona type polymeric nanoparticles and their biomedical applications. Furthermore, we describe the potential of self-assembled nanoparticles composed of γ-PGA hydrophobic derivatives (γ-hPGA) developed by our research group as protein carriers.

2. Preparation of polymeric nanoparticles

2.1. Particle preparation processes

Conventionally, polymeric nanoparticles have been prepared mainly by two methods: (i) the polymerization and polycondensation of monomers, and (ii) the dispersion of preformed polymers [1]. Polymerization methods can be distinguished as: emulsion, dispersion and suspension polymerization, according to the solubility of the monomer and polymer in the dispersion medium. Emulsion polymerization has been extensively studied as a method for preparing nanoparticles [3,24]. This approach is one of the fastest methods for nanoparticle preparation and is readily scalable. Briefly, the hydrophobic monomer is dispersed as emulsion in an aqueous phase, the radical polymerization is initiated in the aqueous phase, polymer particles are nucleated and grow by means of a flux of new monomer from the monomer emulsion droplets. The polymerization course and the final size of the particles are controlled by the addition of the chemical initiator or by the variations in physical parameters with or without the presence of surfactants to stabilize the particles. Particle formation by emulsion polymerization has been primarily developed for the radical polymerization of vinyl monomers such as styrene, acrylates or methacrylates [25].

On the other hand, several methods have been reported to prepare biodegradable nanoparticles from poly(lactic acid) (PLA), poly(lactide-*co*-glycolide) (PLGA), and poly(ε-caprolactone) (PCL) by dispersing preformed polymers [1,4]. In this method, solvent evaporation is a common and convenient method for nanoparticle preparation. The polymer is dissolved in an organic solvent like dichloromethane, chloroform or ethyl acetate, and then emulsified into an aqueous solution to create an oil-in-water (o/w) emulsion by using a surfactant such as poly(vinyl alcohol). After the formation of a stable emulsion, the organic solvent is evaporated by increasing the temperature under pressure. The effect of this process is variable depending on the properties of the nanoparticles.

Amphiphilic block or graft copolymers consisting of hydrophilic and hydrophobic segments are self-assembling materials, and are capable of forming polymeric associates in aqueous solutions. These nanoparticles can be prepared by solvent displacement or direct dispersion method of amphiphilic polymers [18]. Solvent displacement method is based on the precipitation of a dissolved polymer from organic solution and the diffusion of the organic solvent in the aqueous medium. Generally, amphiphilic polymers dissolved water-miscible organic solvents were dialyzed against water to form nanoparticles. Aggregates of various morphologies have been observed in a number of self-assembled polymeric systems. The morphology of the nanoparticles produced from amphiphilic block/graft copolymers can be varied by changing the composition of the hydrophobic and hydrophilic blocks on the polymer chains [26–28]. Amphiphilic block copolymers, such as poly(ethylene glycol)-*b*-poly(lactic acid) (PEG-*b*-PLA) or PEG-*b*-PCL, are very attractive for use as drug delivery applications [29,30].

2.2. Preparation of core-corona type polymeric nanoparticles

In our research group, polymeric nanoparticles with hydrophobic polymer cores and hydrophilic polymer coronas have been simply synthesized by the free radical copolymerization of hydrophilic macromonomers and hydrophobic comonomers in a polar solvent such as alcohol or a water/alcohol mixture [31–48]. The mechanism of nanoparticle formation is shown in Fig. 1. During the polymerization of hydrophilic macromonomers with hydrophobic comonomers in a polar solvent in the presence of a radical initiator, the generated amphiphilic

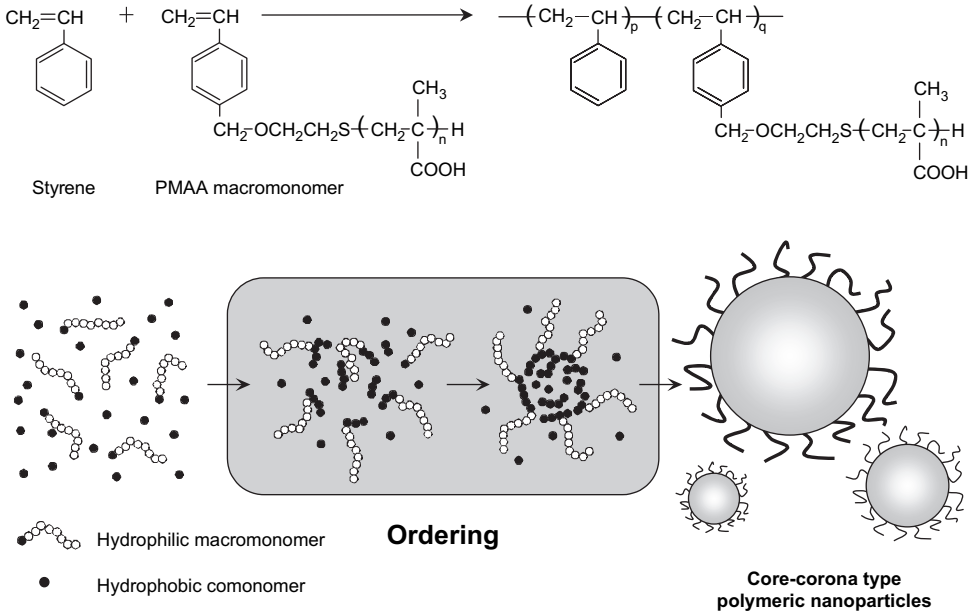

Fig. 1. Mechanism of core-corona type polymeric nanoparticle formation.

copolymers self-assembled in order to form core-corona polymeric nanoparticles, possibly with a hydrophobic core and a hydrophilic graft polymer layer on their surfaces (Fig. 2). Electron spectroscopy for chemical analysis (ESCA), dynamic light scattering (DLS) measurement, and transmission electron microscope (TEM) observations supported the accumulation of a macromonomer component on the surface of the nanoparticles [39,40,46,48]. The size of the nanoparticles, the molecular weight of the graft polymers, and the conversion of polymerization increased with an increase in the reaction time, thus indicating an *in situ* self-assembling process for nanoparticle formation. When PEG macromonomers and methyl methacrylate (MMA) are used as hydrophilic macromonomers and hydrophobic comonomers in water/ethanol mixture, first methacrylate-rich graft copolymers are produced to form a nucleus of the particles, and then MMA is adsorbed in particles similar to dispersion polymerization. PEG branches act as a stabilizer to form stable nanoparticles. Moreover, MMA is easy to come into hydrophobic domain of the particles and propagate. Propagation polymer radicals in the particles are considered to be stable and have a long lifetime. Also, the termination rate of the radicals decreases in the particles, as the viscosity of the polymerization medium increases. Consequently, molecular weight of graft copolymers can be assumed to increase in the last stage of copolymerization [20,31]. Other research groups have also synthesized similar core-corona nanoparticles using the same methodology [49–51].

Their size distributions were also quite narrow and uniform in all cases. The size of the nanoparticles (100 nm to 3 μm) could be controlled by changing the polymerization conditions [43,44]. By designing and synthesizing different functional macromonomers, a variety of water-dispersible nanoparticles

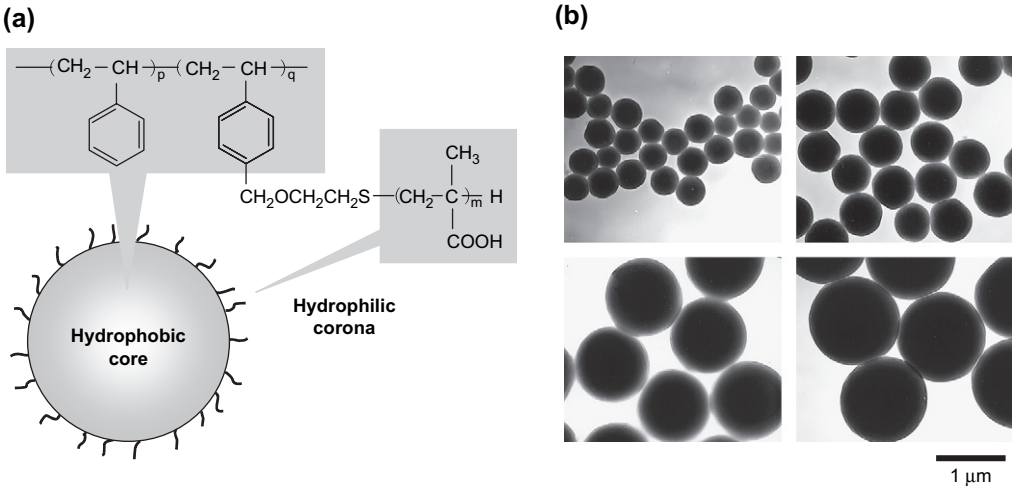

Fig. 2. (a) Structure of core-corona type polymeric nanoparticles. (b) TEM images of nanoparticles.

with functional polymeric branches on their surfaces could be obtained. For instance, we have already developed nanoparticles bearing pH sensitive anionic poly(methacrylic acid) (PMAA) [37], cationic poly(vinylamine) (PVAm) [52], nonionic poly(ethylene glycol) (PEG) [44], thermosensitive poly(*N*-isopropylacrylamide) (PNIPAAm) [39] and poly(*N*-vinylisobutyramide) (PNVIBA) [42]. Regulating the monomers used and the reaction conditions can easily control their surface properties, such as the density or molecular weight of their hydrophilic polymers, the charge or its distribution, and the stimuli responses.

3. Application of core-corona type polystyrene nanoparticles

Core-corona nanoparticles have highly hydrated polymer coronas in the aqueous phase. The surface functionalities (neutral, cationic, anionic, thermoresponsive units) of core-corona nanoparticles can be readily modified by changing the macromonomer. To investigate their potential functions, we have prepared the nanoparticles conjugated with proteins [53], peptides [54], saccharides [55,56], and metal particles [57–62] using functional groups introduced onto the corona. Fig. 3 shows an example of the application of these core-corona nanoparticles.

3.1. Oral peptide delivery by nanoparticles

Nanoparticles have been studied extensively as carriers for oral peptide delivery [63–65]. We evaluated the usefulness of core-corona nanoparticles as carriers for hydrophilic peptide drugs, and their potential as carriers that enhance peptide absorption via the gastrointestinal (GI) tract. Salmon calcitonin (sCT) was used as a model drug to study the oral delivery of peptides, and it is well known that its absorption can be evaluated from the hypocalcemic effect which is only found in the intact form [66].

After the oral administration of mixtures of sCT and nanoparticles to rats, the ionized calcium concentration in the blood obtained from the tail vein was measured. The blood ionized calcium concentration decreased slightly after the oral administration of sCT aqueous solution (Fig. 4). This result suggests that a small amount of intact sCT is absorbed via the GI tract, although the majority is degraded by proteases, and the membrane permeability of the residual intact sCT is very low. We found that sCT absorption via the GI tract is enhanced by the nanoparticles, and that this enhancement was affected by the chemical structure of the macromonomers on the nanoparticle surface. sCT absorption was enhanced most strongly by nanoparticles with PNIPAAm chains on their surfaces (Fig. 4) [67]. PNVA and PEG nanoparticles did not show this enhancement effect on sCT absorption. The absorption of sCT was also enhanced by nanoparticles with surface PMAA or PVAm chains, although the enhancement was weaker than that induced by the PNIPAAm nanoparticles (data not shown).

The hypocalcemic effects after oral administration of mixtures of sCT and nanoparticles were only retained for 4 h, irrespective of the macromonomer structure. This suggests that the absorption amount of sCT was not sufficient for inducing the substantial hypocalcemic effect. We found two ways to improve further this low absorption of sCT. One way is to optimize the administration schedule of the mixture of sCT and PNIPAAm nanoparticles [68]. When the dose of the mixture was halved and one half was given orally 40 min after the other half, the sCT-induced hypocalcemic effect was markedly enhanced by PNIPAAm nanoparticles. The area of the reduction in the blood ionized calcium concentration was about three times that after administration of a single full dose of the same mixture.

The other way to improve sCT absorption is to optimize the chemical structure of the nanoparticles. When styrene was polymerized with two different kinds of macromonomers, polystyrene nanoparticles having two macromonomer chains on their surfaces were obtained [69]. The enhancement effect of

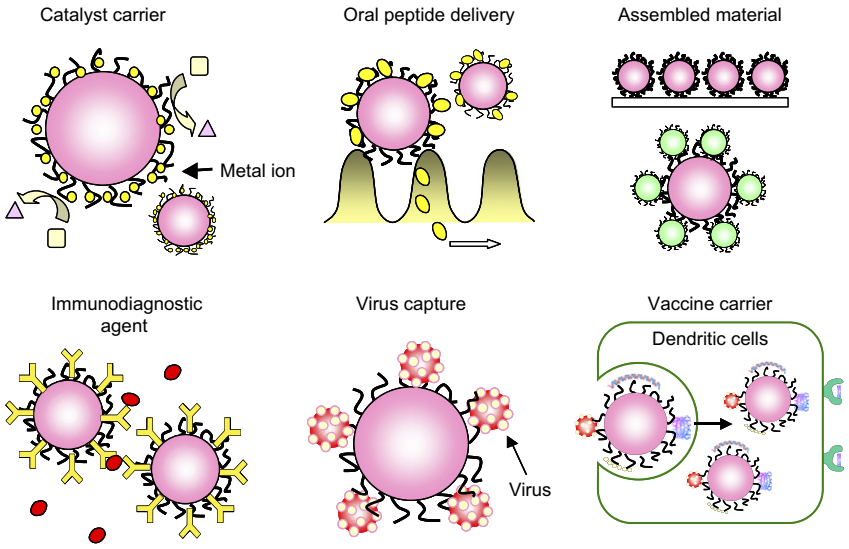

Fig. 3. Applications of core-corona type polymeric nanoparticles.

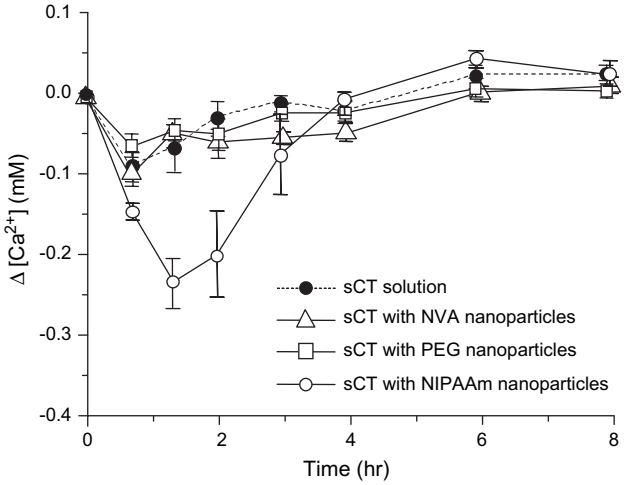

Fig. 4. Concentration–time profiles of ionized blood calcium levels after the oral administration of sCT aqueous solution, a mixture of sCT and NVA nanoparticles, a mixture of sCT and PEG nanoparticles, and a mixture of sCT and PNIPAAm nanoparticles in rats (0.25 mg sCT/2.5 ml dosing solution/kg rat). The nanoparticle concentration in the dosing solution was 10 mg/ml. The PNIPAAm nanoparticle size and molecular weight of the macromonomers were 750 nm and 3500, respectively. Each value represents the means ± SE. Data from Ref. [67].

sCT absorption by PNIPAAm nanoparticles was increased considerably by introducing cationic PVAm chains to their surfaces. The area of the reduction in the blood ionized calcium concentration was increased by about three-fold. On the other hand, the introduction of nonionic PNVA chains eliminated completely the absorption-enhancing function of PNIPAAm nanoparticles. It has been confirmed that nanoparticles having surface PNVA and PMAA chains have no charge, irrespective of the ratio of anionic PMAA chains. PNVA chains probably shield the other functional groups on the same nanoparticle surface. It seems that this shield prevented the PNIPAAm groups from enhancing sCT absorption.

3.2. Mechanism of peptide delivery by nanoparticles

It has been reported that mucoadhesive polymers improve the bioavailability of poor absorptive drugs [70]. We have examined the mechanism of the enhancement effect of sCT absorption by these nanoparticles in detail and proved that the absorption enhancement results mainly from both mucoadhesion of nanoparticles incorporating sCT in the GI tract and an increase in the stability of sCT against degradation by digestive enzymes [71–73].

The GI transit time of each radiolabeled type of nanoparticles in rats indicated that PNIPAAm, PVAm and PMAA nanoparticles adhered to the GI mucosa, and that PNVA nanoparticles did not have the mucoadhesive property. The mucoadhesive strength of PNIPAAm nanoparticles was stronger than those of PVAm and PMAA nanoparticles in the *in situ* experiments. The mucoadhesive property of nanoparticles appears to be related to the absorption enhancement of orally administered sCT because there was a good correlation between the strength of mucoadhesion and the effect of the *in vivo* absorption enhancement [71]. On the other hand, nanoparticles protected sCT against digestive enzyme-catalyzed degradation in an *in vitro* study. This stabilizing effect was affected by the chemical structure of the hydrophilic polymeric chains on the nanoparticle surface. There was a good correlation between the *in vitro* stability of sCT in the presence of nanoparticles and the ranking of the *in vivo* effectiveness of nanoparticles for enhancing the absorption of sCT [72]. It was concluded that the absorption enhancement of sCT by nanoparticles resulted from both the mucoadhesion of nanoparticles incorporating sCT onto the intestinal mucosa, and an increase in the stability of sCT against digestive enzymes.

3.3. Immobilization of proteins onto the nanoparticles

Polymeric micro/nanoparticles have an extremely large specific surface, and are frequently used for the immobilization of biomolecules such as antibodies and enzymes in order to create immunoassays [74] and catalytic systems [58]. Enzymes are immobilized onto or into the particles to increase their thermostability, operational satiability, and recovery [75].

Core-corona nanoparticles have highly hydrated polymer coronas with functional groups in the aqueous phase, allowing the covalent conjugation of biomolecules such as proteins. Thus, we investigated the immobilization of lectins onto PMAA-covered polystyrene nanoparticles, and their capture of human immunodeficiency virus type 1 (HIV-1) through affinity interaction between the gp120 mannose and the immobilized lectins. The mean diameters of the nanoparticles used were 310, 360, 660, 940, and 1230 nm. Nanoparticles of different sizes showed a strongly negative zeta potential (−35 mV) in phosphate-buffered saline (PBS). This could be attributed to the presence of ionized carboxyl groups from the graft chains on the nanoparticle surfaces.

Concanavalin A (Con A) was also covalently immobilized to the nanoparticles (Fig. 5a). The carboxyl groups of the nanoparticle surface were first activated by 1-ethyl-3-(3-dimethyl aminopropyl) carbodiimide (WSC) and were mixed with Con A in PBS. Con A was immobilized onto the nanoparticles by amide bonds between carboxyl groups on the nanoparticle surfaces and Con A amide groups. Fig. 5b and c shows the amount of Con A immobilized onto nanoparticles of different sizes by covalent binding [76]. The amount of immobilized Con A increased upon increasing the concentration of Con A. The efficiency of Con A immobilization using WSC reached about 50% at maximum. The amount of Con A immobilized per nanoparticle unit weight showed a different tendency based on the size of the nanoparticles (Fig. 5b); the amount of covalently immobilized Con A increased upon decreasing the size of the nanoparticles. These differences can be attributed to the surface area per unit weight of the nanoparticles. The surface area of the nanoparticles per milligram was 159, 87, 61, and 47 cm^2 for the 360, 660, 940, and 1230 nm sized nanoparticles, respectively. The amount of Con A immobilized per unit surface area (cm^2) did not differ significantly according to the size of the nanoparticles

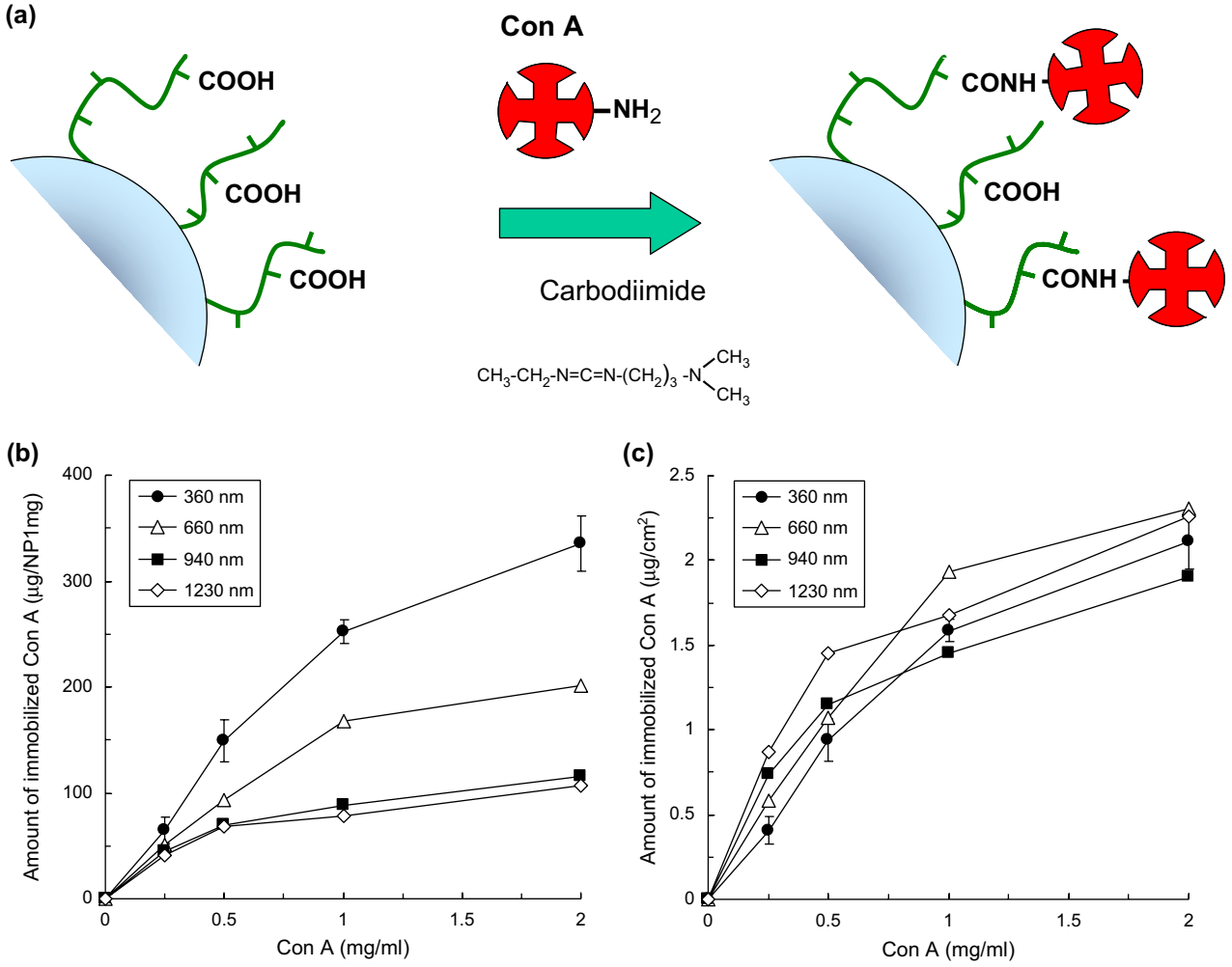

Fig. 5. Immobilization of concanavalin A (Con A) onto the surface of nanoparticles (a). Effect of the particle size on the amount of Con A immobilized onto nanoparticles (NP). NP were treated with WSC and Con A was mixed to a final concentration of 0.25–2 mg/ml. The amount of immobilized Con A was calculated by the immobilized Con A weight (μg)/NP weight (1 mg) (b), and the immobilized Con A weight (μg)/surface area of NP (cm^2) (c). Data from Ref. [76].

(Fig. 5c) [76]. These results demonstrate that the amount of immobilized Con A was significantly dependent on the surface area of the particle. Nano-sized particles appeared to be more effective for loading proteins when compared to micro-sized particles.

3.4. Virus capture by Con A-immobilized nanoparticles

HIV-1 is a spherical RNA virus with a diameter of 100 nm and possesses an envelope containing the glycoprotein gp120. Con A recognizes the gp120 on the HIV-1 surface, in particular the mannose residues of the oligosaccharide chains [77]. It was reported that the HIV-1 envelope glycoprotein could be purified by Con A–agarose affinity chromatography [78]. Thus, it is possible that gp120 and HIV-1 particles can be effectively captured by these lectins, if they are ideally immobilized onto certain materials such as micro/nanoparticles.

To investigate the capability of virus capture by Con A-immobilized PMAA nanoparticles (Con A-NP), Con A-NP of different sizes were mixed with an HIV-1 suspension in medium. The amount of captured HIV-1 was determined by the residual gp120 antigen level and the viral infectivity in the supernatants after centrifugation. Fig. 6 shows the capture efficiency of inactivated HIV-1 by Con A-NP of different sizes [76]. A dose-dependent increase of capture efficiency was observed with increasing concentrations of Con A. However, no significant differences in capture efficiency were found among the different particle sizes. This result indicates that capture efficiency of Con A-NP depends on the amount of immobilized Con A. The size of the Con A-NP was increased to about 200 nm when the HIV-1 particles and gp120 antigens were captured, and slight aggregation was observed (data not shown). This aggregation is attributed to the crosslinking of Con A-NP by the HIV-1 particles and gp120 antigens [53,79].

Con A-NP of different sizes could equally capture inactivated HIV-1. It was reported that enzymes immobilized onto micro/nanospheres had a lower apparent affinity for their substrates than the free enzyme [80,81]. This phenomenon may be attributed to the steric hindrance of the active site by the nanoparticles, the loss of enzyme flexibility necessary for substrate binding, or denaturation of the immobilized enzyme by coupling reactions. Thus, the possibility exists that a loss of

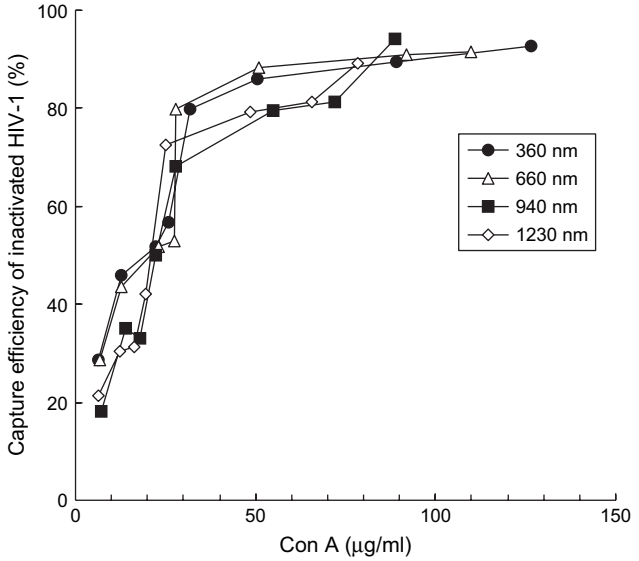

Fig. 6. Effect of the particle size on the capture efficiency of HIV-1 with Con A-NP. Various concentrations of Con A-NP of different sizes and inactivated HIV-1 suspension were mixed, and incubated for 24 h at 4 °C. After incubation, the supernatants were collected and the residual gp120 antigen levels were determined by ELISA. The capture efficiency for HIV-1 with Con A-NP was calculated by: (residual gp120 antigen/initial concentration of gp120) × 100. Data from Ref. [76].

binding activity of Con A immobilized onto the nanoparticles may be caused by steric hindrance of the mannose binding sites, or denaturation. However, Con A-NP could efficiently capture inactivated HIV-1 and the capture efficiency for inactivated HIV-1 was similar in all cases tested. These results suggest that the size of the nanoparticles (300–1200 nm) does not significantly influence the mannose binding activity of Con A.

3.5. Development of an anti-HIV-1 vaccine using HIV-1-capturing nanoparticles

The development of a prophylactic/therapeutic HIV-1 vaccine based on recombinant proteins is needed for the control of the worldwide spread of the acquired immune deficiency syndrome (AIDS) epidemic. Subunit protein and peptide vaccines are generally very safe with well-defined components. However, these antigens are often poorly immunogenic and thus require the use of adjuvants to induce adequate immunity [82,83].

Particulate adjuvants (e.g. micro/nanoparticles, emulsions, ISCOMS, liposomes, virosomes, and virus-like particles) have been widely investigated as HIV-1 vaccine delivery systems [84]. The adjuvant effect of the micro/nanoparticles appears to be largely a consequence of their uptake into antigen-presenting cells (APC). More importantly, particulate antigens have been shown to be more efficient than soluble antigens for the induction of immune responses [85,86]. There are several factors that can affect the immune response induced by immunization with particulate antigens. Among them are the particle sizes, the chemical structure of the particles, their surface hydrophilicity, zeta potential, and adjuvants used within the formulations.

To that end, we focused on the development of an HIV-1 vaccine using HIV-1-capturing Con A-NP (HIV-NP) [76,87–90]. Various strategies for immunization with HIV-NP (350 nm) were undertaken to induce an HIV-1-specific IgA response in the mouse genital tract. HIV-NP were administered intravaginally, orally, intranasally or intraperitoneally to these mice. As shown in Fig. 7, intranasal immunization with HIV-NP was more effective as compared with the other immunization routes in terms of a vaginal IgA response [88]. In addition, vaginal washes from intranasally immunized mice were capable of neutralizing HIV-1_{IIIB}. Thus, the application of HIV-NP is a practical approach to promote HIV-1-specific IgA response from the mouse vaginal mucosa, and the intranasal route appears to be an effective immunization strategy in this animal model.

To examine whether these results would translate to a non-human primate model and whether the generated immunity was protective, we used the rhesus macaque/SHIV system. Three macaques were intranasally immunized with Con A-NP or inactivated SHIV KU-2-capturing nanoparticles (SHIV-NP). Moreover, to determine whether the intranasal immunization would have a protective effect against an intravaginal challenge with pathogenic SHIV KU-2, all of the macaques were vaginally inoculated with SHIV KU-2. Intranasal immunization with SHIV-NS could effectively induce HIV-1-specific antibody responses. After the intravaginal challenge, viral RNA loads in the plasma were much lower in the SHIV-NP-immunized macaque than in the control macaque (data not shown) [90]. Thus, SHIV-NP-immunized macaques exhibited partial protection against vaginal and systemic challenges with SHIV KU-2. These results may be helpful for the development of a vaccine against AIDS.

4. Preparation of biodegradable nanoparticles based on amphiphilic poly(amino acid)

Numerous investigators have shown that the biological distribution of drugs, proteins and DNA can be modified, both at the cellular and organ levels, using micro/nanoparticle delivery systems. Recently, many studies have focused on self-assembled biodegradable nanoparticles for biomedical and pharmaceutical applications. In particular, poly(amino acid)s have received considerable attention for their medical applications as potential polymeric drug carriers. Several amphiphilic block and graft copolymers based on poly(amino acid) have been employed such as poly(L-glutamic acid) [91], poly(L-aspartic acid) [11,92], poly(L-lysine) [93,94], poly(L-arginine) [95], poly(L-asparagine) [96], and poly(γ-glutamic acid) [97–99] as hydrophilic segments, and poly(β-benzyl-L-aspartate) [100], poly(γ-benzyl-L-glutamate) [101], and poly(L-histidine) [102] as hydrophobic segments. Amphiphilic copolymers based on poly(amino acid) form micelles through self-association in water. The formed micelles can act as hydrophobic drug carriers such as for the anticancer agent adriamycin. Enhanced tumor accumulation, long blood circulation times, and effective treatment of solid tumors of those drug-load micelles have been reported [100].

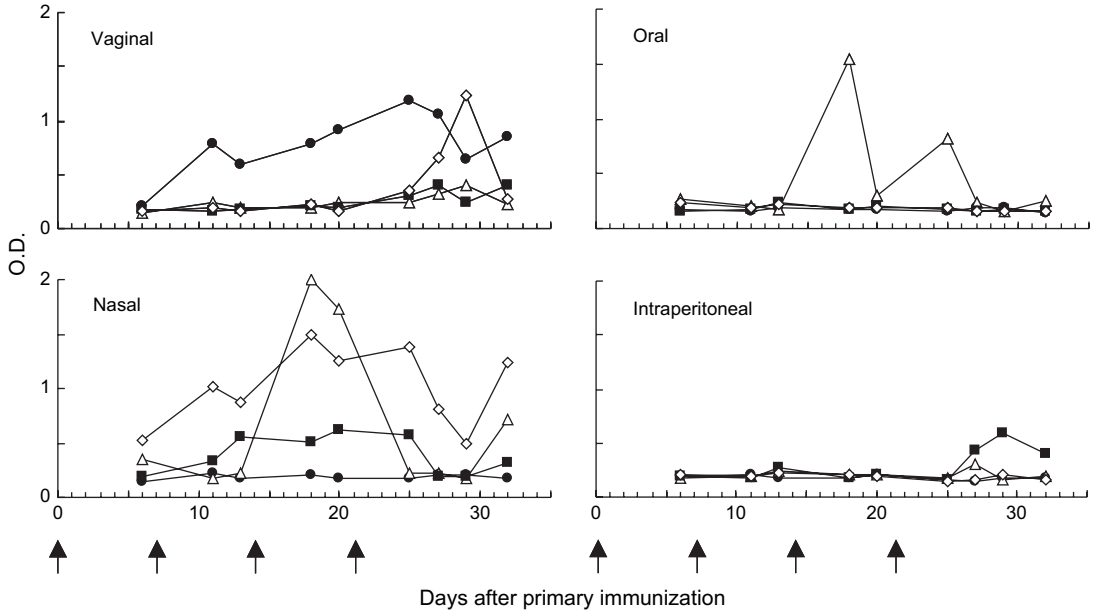

Fig. 7. Anti-HIV-1 gp120 IgA antibody levels in vaginal washes following intravaginal, oral, intranasal, or intraperitoneal immunization with HIV-NP (350 nm). The levels of gp120 V3-specific IgA and IgG antibodies were measured by ELISA. The results from four individual mice per group are shown. The specific absorbance of the vaginal washes collected from Con A-NP-immunized mice was <0.25 O.D. Arrows indicate the time of immunization. Data from Ref. [88].

We have studied the synthesis and clinical applications of core-corona polymeric nanoparticles composed of hydrophobic polystyrene and hydrophilic macromonomers. However, both biodegradability and biocompatibility are required for medical use. Therefore, the development of biodegradable nanoparticles is indispensable for these applications. To this end, we prepared novel biodegradable nanoparticles composed of hydrophobically modified poly(γ-glutamic acid) (γ-PGA).

4.1. Synthesis of γ-PGA hydrophobic derivatives

γ-PGA is a bacterially produced, water-soluble polyamide, which is the object of current interest because of its natural origin and biodegradability [103–105]. This polymer is different from proteins in that peptide linkages are formed between the α-amino and the γ-carboxylic acid groups. It is a high molecular weight polypeptide composed of γ-linked glutamic acid units, and its α-carboxylate side chains can be chemically modified. We also developed a modified method to prepare γ-PGA as a drug delivery carrier [106], a tissue engineering material [107], and a thermosensitive polymer [108].

γ-PGA hydrophobic derivatives (γ-hPGA) were synthesized by the covalent attachment of L-phenylalanine ethylester (L-PAE) to γ-PGA via an amide bond (Fig. 8). γ-PGA is a hydrophilic segment which has biodegradable components containing carboxyl functional groups at the side chains. L-PAE is a hydrophobic segment and was chosen as a nontoxic amino acid. γ-PGA (number-average molecular weight, $M_n = 380{,}000$, D/L ratio = 6:4, $pK_a = 2.3$) was hydrophobically modified by L-PAE in the presence of WSC in 50 mM $NaHCO_3$ (pH 8.5) for 24 h at room temperature. The resulting solutions were then dialyzed against distilled water using cellulose membrane tubing (50,000 molecular weight cut off) for 72 h at room temperature. The dialyzed solutions were then freeze dried. The degree of grafting of L-PAE was determined by ^1H NMR using integrals of the methylene peaks of γ-PGA and the phenyl group peaks of phenylalanine (Fig. 9). Graft copolymers with different degrees of L-PAE grafting were prepared by changing the molar ratio of the glutamic acid units of γ-PGA to WSC (Table 1). WSC reacts with the carboxyl groups of γ-PGA to form an active ester intermediate, which then reacts with a primary amine group from L-PAE to form an amide bond. The degree

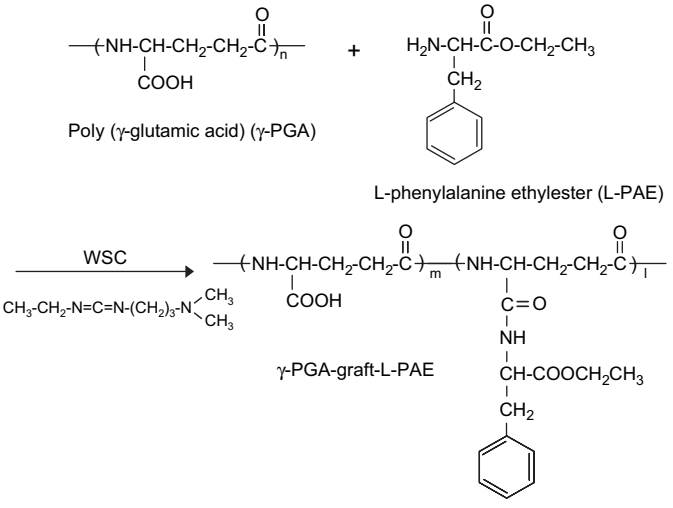

Fig. 8. Chemical structure of γ-PGA and synthesis scheme for γ-PGA-*graft*-L-PAE (γ-PGA hydrophobic derivatives).

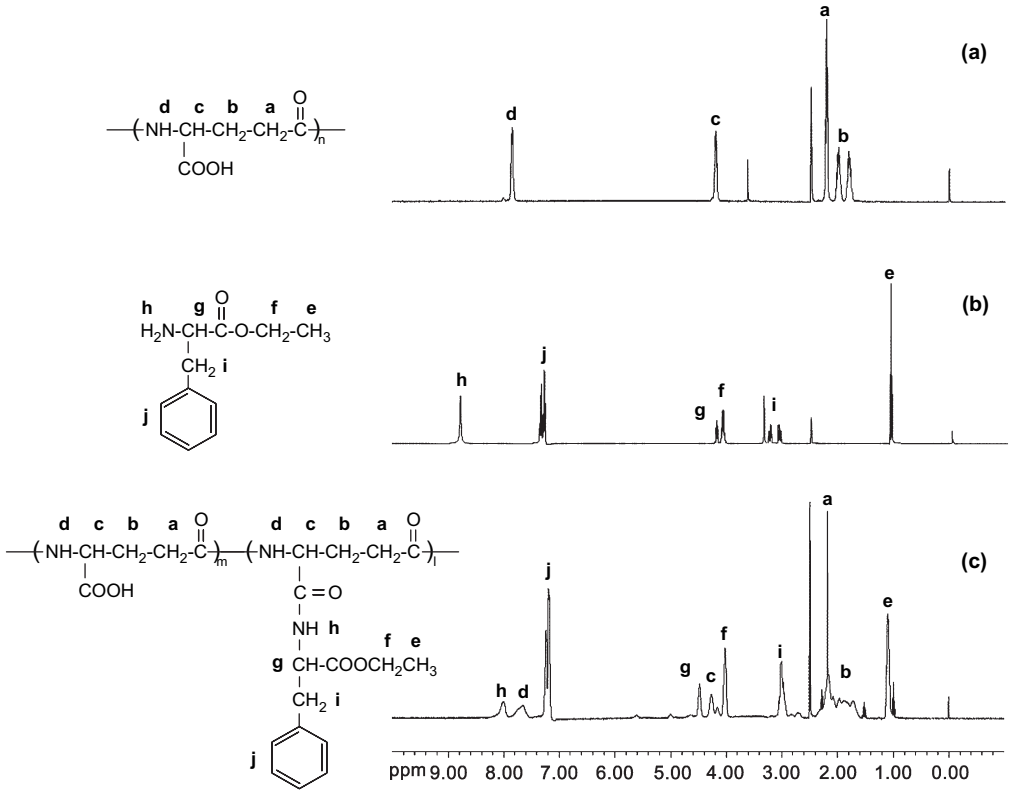

Fig. 9. ^{1}H NMR spectra of γ-PGA (a), L-PAE (b), and γ-PGA-*graft*-L-PAE-53 (c) at 80 °C in DMSO-d_6.

of L-PAE grafting can be easily controlled by altering the amount of WSC [21,22].

4.2. Preparation of γ-hPGA nanoparticles

Amphiphilic block/graft copolymers can self-aggregate in aqueous solution due to their intra- and/or intermolecular hydrophobic interactions [109,110]. Therefore, γ-hPGA nanoparticles composed of γ-PGA-*graft*-L-PAE were prepared by a precipitation and dialysis method. γ-PGA-*graft*-L-PAE (10 mg) was dissolved in 1 ml of DMSO, followed by the addition of saline at the same volume as the solvent to yield a translucent solution. The solutions were then dialyzed against distilled water using cellulose membrane tubing (50,000 molecular weight cut off) to form the nanoparticles and to remove the organic solvents for 72 h at room temperature. The size distribution and surface charge of the γ-hPGA nanoparticles in aqueous media were then measured by dynamic light scattering (DLS) and zeta potential measurements.

Table 1
Synthesis of γ-PGA-*graft*-L-PAE copolymers

Run	γ-PGA (unit mmol)	L-PAE (mmol)	WSC (mmol)	Yield (%)	Grafting degree[a] (%)
1	4.7	4.7	0.5	50	10
2	4.7	4.7	1.2	50	18
3	4.7	4.7	2.4	58	23
4	4.7	4.7	3.5	52	36
5	4.7	4.7	3.8	56	43
6	4.7	4.7	4.2	59	49
7	4.7	4.7	4.7	64	53
8	4.7	4.7	5.2	61	61
9	4.7	4.7	9.4	65	64

[a] Grafting degree of L-PAE was measured by ^{1}H NMR.

γ-PGA-*graft*-L-PAE could form nanoparticles due to its amphiphilic characteristics. Fig. 10 shows a representative size distribution (a) and zeta potential plot (b) of nanoparticles prepared from γ-PGA-*graft*-L-PAE with a 53% grafting degree (γ-PGA-NP-53) in PBS [111]. The mean diameter and zeta potential of γ-hPGA nanoparticles of various L-PAE grafting degrees are summarized in Table 2. These nanoparticles could be prepared from γ-PGA-*graft*-L-PAE with 43–61% L-PAE grafting. The size of the γ-hPGA nanoparticles decreased with an increasing degree of L-PAE grafting [111]. This increased grafting may enhance the hydrophobic interactions between the L-PAE groups attached to the γ-PGA backbone, resulting in an increased stability of the hydrophobic cores. Thus, the size of the γ-hPGA nanoparticles can be controlled by the degree of L-PAE grafting. However, γ-PGA-*graft*-L-PAE with a low L-PAE grafting of 10–36% could not form nanoparticles due to the weak interactions between the L-PAE groups attached to the γ-PGA backbone. These graft copolymers were dissolved in water. The γ-hPGA nanoparticles showed a highly negative zeta potential in PBS. However, the zeta potential seemed to be independent of the grafting degree (Table 2) [111]. Fig. 11 shows scanning electron microscope (SEM) images of the γ-PGA-NP-53. These nanoparticles were spherical in shape and the sizes of the nanoparticles

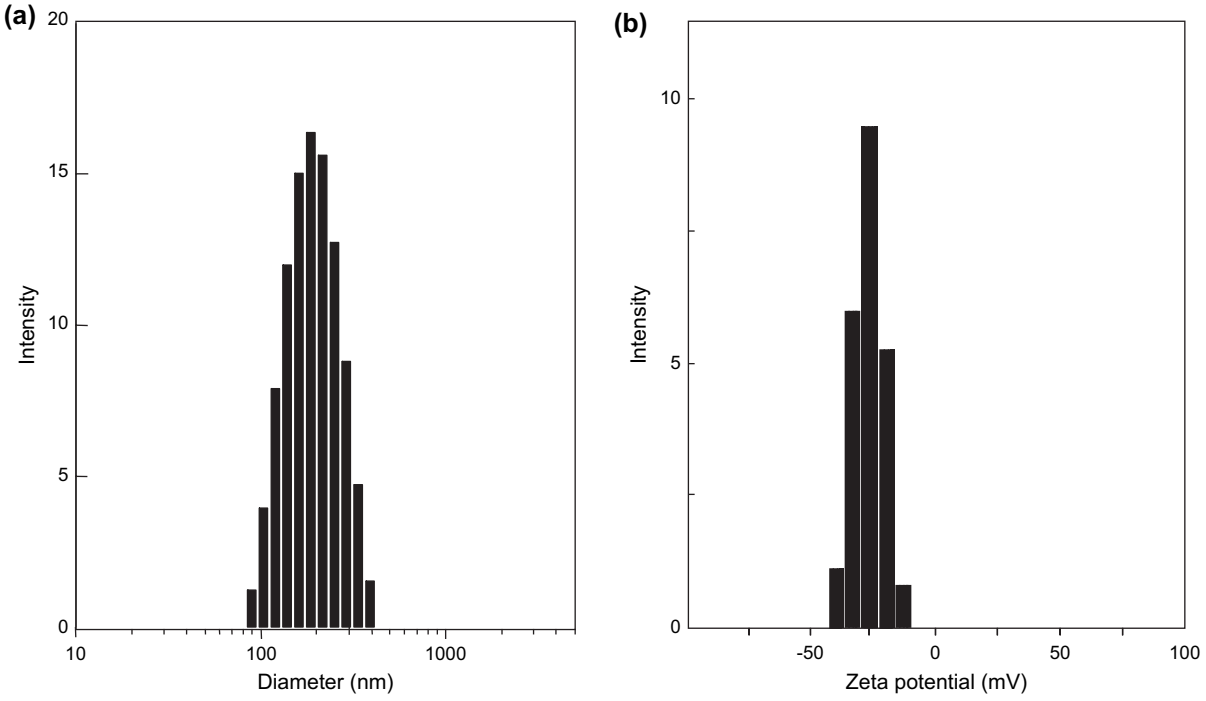

Fig. 10. Particle size (a) and surface charge (b) of γ-hPGA nanoparticles (γ-PGA-NP-53) measured by DLS and zeta potential measurements. Data from Ref. [111].

observed by SEM were in agreement with the results of the DLS measurements.

4.3. Characterization of γ-hPGA nanoparticles

Hydrophobic domains in the γ-hPGA nanoparticles were detected with the Coomassie Brilliant Blue (CBB) G-250 dye. CBB is highly soluble in water, but also possesses a marked hydrophobic character, mainly due to the presence of six aromatic rings. This molecule may thus participate in strong hydrophobic interactions. Moreover, its wavelength of maximum absorption is shifted from 584 nm in polar media to 618 nm in nonpolar media [112]. Thus, in this experiment, CBB was used as a probe of its microenvironment polarity.

The absorption spectra of CBB in nanoparticle (γ-PGA-NP-53) solutions of different concentrations are shown in Fig. 12. The maximum absorption peak of CBB was shifted towards higher wavelengths when the nanoparticles' concentration was increased. However, for the unmodified γ-PGA or L-PAE monomer (dissolved in PBS) alone, the absorbance remained constant (data not shown). These results suggest that the maximum absorption change in the case of γ-hPGA nanoparticles can be attributed to the presence of hydrophobic domains. These hydrophobic domains probably result from the intra- or intermolecular associations of L-PAE attached to

Table 2
Particle size and zeta potential of γ-hPGA nanoparticles composed of various L-PAE grafting degrees

Run	Grafting degree (%)	Particle size[a] (nm)	C.V.[b] (%)	Zeta potential[a] (mV)
1	10	No particles	–	–
2	18	No particles	–	–
3	23	No particles	–	–
4	36	No particles	–	–
5	43	305	26.3	−24.5
6	49	271	26.2	−23.8
7	53	200	24.1	−26.3
8	61	152	20.1	−24.4
9	64	Aggregation	–	–

Data from Ref. [111].
[a] Particle size and zeta potential of γ-hPGA nanoparticles were measured in PBS by a Zetasizer nano ZS.
[b] C.V. (coefficient of variation) = SD (standard deviation)/mean diameter.

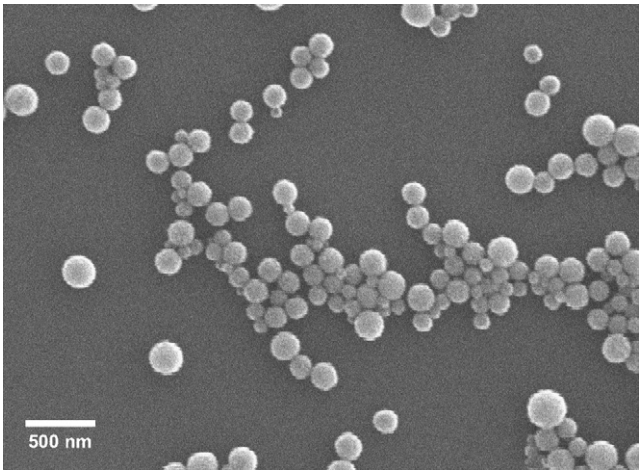

Fig. 11. SEM images of γ-hPGA nanoparticles (γ-PGA-NP-53).

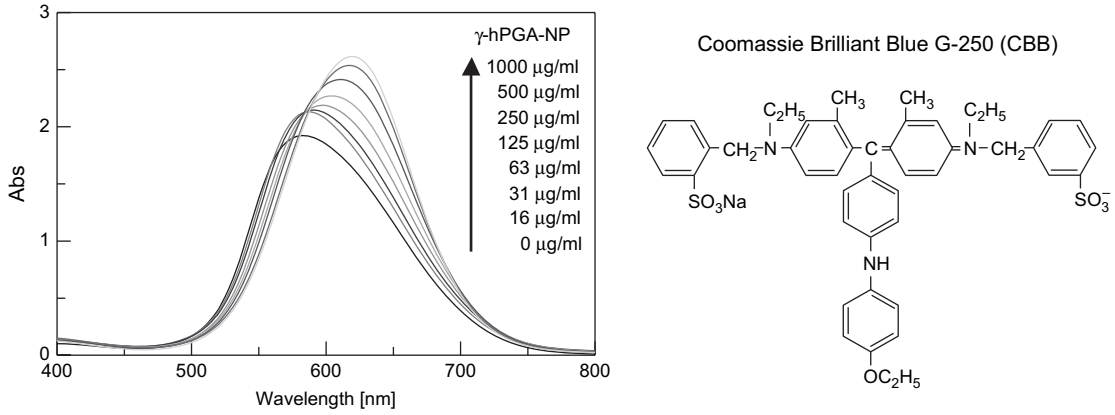

Fig. 12. Absorption spectra of CBB (0.05 mM) in PBS with various concentrations of γ-hPGA nanoparticles (γ-PGA-NP-53).

γ-PGA. The specific self-assembly behavior of γ-PGA-*graft*-L-PAE in aqueous solution is due to multiple phenyl group stacking [111,113–115].

To investigate the distribution of carboxyl groups on the surface, the γ-hPGA nanoparticles were suspended in buffers of varying pH values (pH 3–11), and the zeta potential was then determined. The zeta potential did not change at pH from 4 to 8. However, it increased with a decrease in pH from 3 to 4 and reached to −7 mV at pH 3.5 (Fig. 13). The nanoparticles below pH 3.5 formed aggregates. This change in the zeta potential was due to the ionization of the carboxyl groups of γ-PGA located near the surface [113]. These results suggest that the structure of the nanoparticles is a core–shell type, with an L-PAE core and an outer γ-PGA cortex. The γ-hPGA nanoparticles were stably dispersed in PBS for a month. Furthermore, freeze-dried samples could be re-dispersed in aqueous solution and reproduced the same particle size. Moreover, *in vitro* cytotoxicity testing showed that the present nanoparticles did not induce any cytotoxicity against HL-60 cells [113].

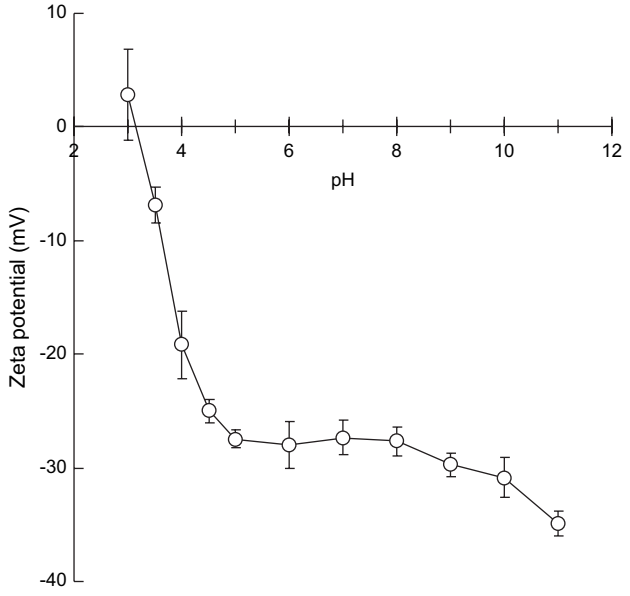

Fig. 13. Changes in the zeta potential of γ-hPGA nanoparticles (γ-PGA-NP-53) as a function of pH. The measurements of the zeta potential were carried out in 50 mM buffer at various pH values (pH 3–11, pH 3–5: citrate; pH 6–8: phosphate citrate; pH 9–11: carbonate).

5. Biodegradability of γ-hPGA nanoparticles

The biodegradation rate of nanoparticles and the release kinetics of loaded drugs can be controlled by their composition ratio, and by the molecular weight of the polymer and graft or block copolymers [116–119]. Therefore, a study of the degradation kinetics is important for biodegradable polymers. However, the degradation properties of nanoparticles prepared from amphiphilic polymers have been studied by only a few research groups [120,121]. It has also been reported that the rate of enzymatic degradation of a polypeptide and its derivatives is dependent upon the hydrophobicity, D/L-isomer composition, conformation (α-helix and random coil), and modifications of the side chains of the polymer [122–125].

5.1. Hydrolytic degradation behavior of γ-hPGA nanoparticles

The biodegradability of γ-PGA and γ-hPGA nanoparticles was estimated from the decrease in their molecular weight following hydrolytic degradation. The hydrolysis of γ-PGA has been investigated in detail. Fan et al. investigated the hydrolysis of γ-PGA in different pH solutions [126]. When γ-PGA was incubated in a neutral buffer at 37 °C, only approximately 10% of the polymer had been hydrolyzed after 60 days. Goto et al. also reported the effects of temperature on the hydrolysis of γ-PGA [127]. The rate of hydrolysis could be accelerated with an increase in the temperature.

The hydrolysis of γ-PGA, γ-PGA-*graft*-L-PAE-10, and γ-PGA-NP-53 was carried out at 80 °C in phosphate buffer (pH 7.4 and 12) as an acceleration test. Three samples with different hydrophobicities were used to study the effect of the hydrophobicity of the polymer on the hydrolytic degradation behavior. After 6, 12, 24, and 48 h, the degraded samples of γ-PGA and its derivatives were analyzed using GPC. Fig. 14 shows the increase in the degradation ratio versus the hydrolysis time at pH 7.4 (a) and 12 (b) [111,115]. An increase in the hydrolysis ratio was observed for the three

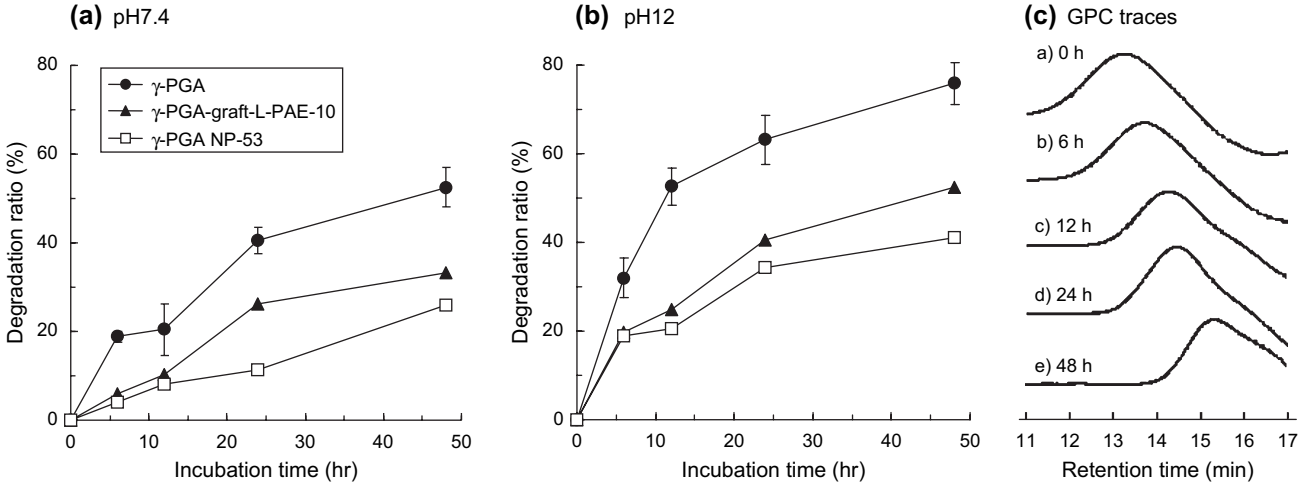

Fig. 14. Degradation of γ-PGA, γ-PGA-*graft*-L-PAE-10 and γ-hPGA nanoparticles (γ-PGA-NP-53) by hydrolysis for different incubation periods in pH 7.4 (phosphate) (a), pH 12 (Na_2HPO_4/NaOH) (b), and GPC traces of γ-PGA with different standing periods in pH 7.4 at 80 °C (c). The degradation ratio was calculated as: $[(M_{n_0} - M_{n_t})/M_{n_0}] \times 100$, where M_{n_0} and M_{n_t} are the number-averaged molecular weight prior to degradation and the M_n at time "t" of degradation, respectively. The results for γ-PGA are presented as means ± SD ($n = 3$). Data from Refs. [111,115].

polymers at both pH values. The hydrolysis ratios of hydrophobically modified γ-PGA were much lower than those of unmodified γ-PGA at both pH values. The introduction of L-PAE groups into γ-PGA delayed the polymer hydrolysis. This could be attributed to the hydrophobicity of γ-PGA. It can be assumed that water molecules cannot easily attack the γ-PGA-NP-53 in comparison to γ-PGA. The hydrolysis of the polymer was thus limited by the rate of penetration and diffusion of water into the core of the nanoparticles [128]. Moreover, the polymer hydrolysis ratio was higher at pH 12 as compared to pH 7.4. This result suggests that the pH is an important factor for the degradation of γ-PGA and its derivatives. Kubota et al. reported the alkaline hydrolysis of γ-PGA [129] and observed that the hydrolysis of γ-PGA was accelerated by the addition of NaOH. The introduction of L-PAE into γ-PGA also influenced the hydrolysis ratio of the polymer. Consequently, the hydrolysis ratio of γ-PGA-NP-53 was lower than that of γ-PGA.

5.2. Enzymatic degradation of γ-hPGA nanoparticles

The enzymatic degradation of γ-PGA nanoparticles was evaluated with γ-glutamyl transpeptidase (γ-GTP). γ-GTP catalyzes the transfer of the γ-glutamyl moiety of γ-glutamyl compounds, such as glutathione, to various amino acids and peptide acceptors. It was observed that γ-PGA was hydrolyzed to glutamic acids by γ-GTP [130].

The enzymatic degradation of γ-PGA, γ-PGA-NP-53, γ-PGA-NP-74, and poly-L-glutamic acid (α-PGA) was examined using γ-GTP. Four samples of the polymer were used to study the effects of the degree of L-PAE grafting on the degradation or disruption of the nanoparticles with γ-PGA as the main chain. After 2, 4, 6, 12, 24, and 48 h, the degraded samples of the polymer were analyzed by GPC. Fig. 15 shows the time dependence of the increased degradation ratio during degradation with γ-GTP [111,115]. The degradation ratio of γ-PGA and γ-PGA derivatives was found to be dependent on the degradation time. In contrast, α-PGA was not degraded by γ-GTP. γ-PGA and γ-PGA-NP-53 did not show any significant differences in their degradability after 48 h of incubation with γ-GTP. However, the degradation of γ-PGA-NP-74 was slower than that of γ-PGA. The increased grafting degree of L-PAE may have enhanced the hydrophobic interactions between the L-PAE groups attached to the γ-PGA backbone, thus resulting in an increased packing and stability of the hydrophobic core. It is hypothesized that the core of the nanoparticle was formed not only by L-PAE, but also by a γ-PGA from the main chain because of the graft copolymer with a short hydrophobic domain [111]. Therefore, it is suggested that γ-PGA incorporated into the core is resistant to degradation by γ-GTP.

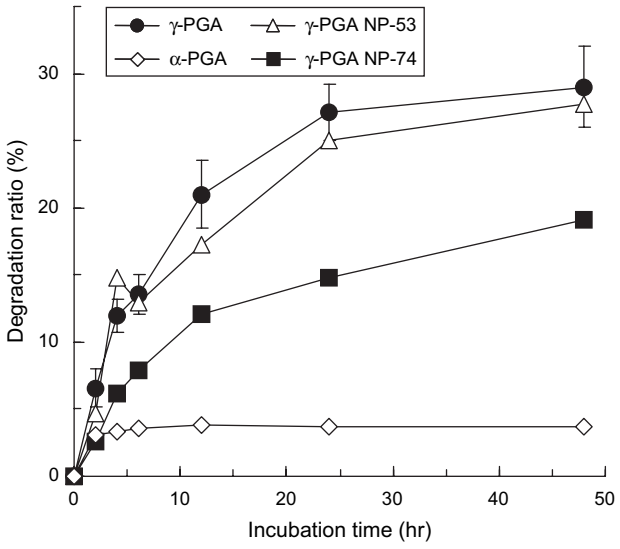

Fig. 15. Degradation of γ-PGA, γ-hPGA nanoparticles (γ-PGA-NP-53, -73) and α-PGA by γ-GTP for different incubation periods at 37 °C. The degradation ratio was calculated as: $[(M_{n_0} - M_{n_t})/M_{n_0}] \times 100$, the results for γ-PGA are presented as means ± SD ($n = 3$). Data from Ref. [115].

Next, four enzymes [Pronase E (PE), protease from *Aspergillus sojae* (protease), cathepsin B (CB), and lipase] were selected for the enzymatic degradation of γ-PGA, γ-PGA-NP-53, and α-PGA. Three samples of the polymer were used to study the cleavage of the amide bond between the α-carboxylate side chain of γ-PGA and L-PAE. PE is a serine protease complex derived from bacteria. CB belongs to the family of cysteine proteases and has been found in various cells. It is involved in the intracellular digestion of extracellular proteins taken in by endocytosis.

The enzymatic degradation studies were carried out *in vitro* at 37 °C in phosphate buffer containing each enzyme. Fig. 16 shows the degradation ratio after enzymatic degradation for 0, 2, 4, 6, 12, and 24 h with PE (a), protease (b), CB (c), and lipase (d) [115]. α-PGA was degraded rapidly by PE, protease and CB, but slowly by lipase. In contrast, γ-PGA was only affected by lipase. It has been reported that γ-PGA was not easily degraded by proteases, such as papain, pepsin, or bromelain [105,131]. In the case of γ-PGA-NP-53, a decrease in the molecular weight of γ-PGA-*graft*-L-PAE was observed with all enzymes tested. There are two possible cleavage sites on γ-PGA-*graft*-L-PAE. One is the amide bond of the γ-PGA composed of γ-linked glutamic acids, and the other is the amide bond between the α-carboxylate side chains of γ-PGA and L-PAE. When L-PAE introduced into γ-PGA is cleaved completely, the molecular weight decreases by about 50%. From Fig. 16, it can be seen that the cleavage of γ-PGA occurred with lipase, and that the cleavage of the amide bond between

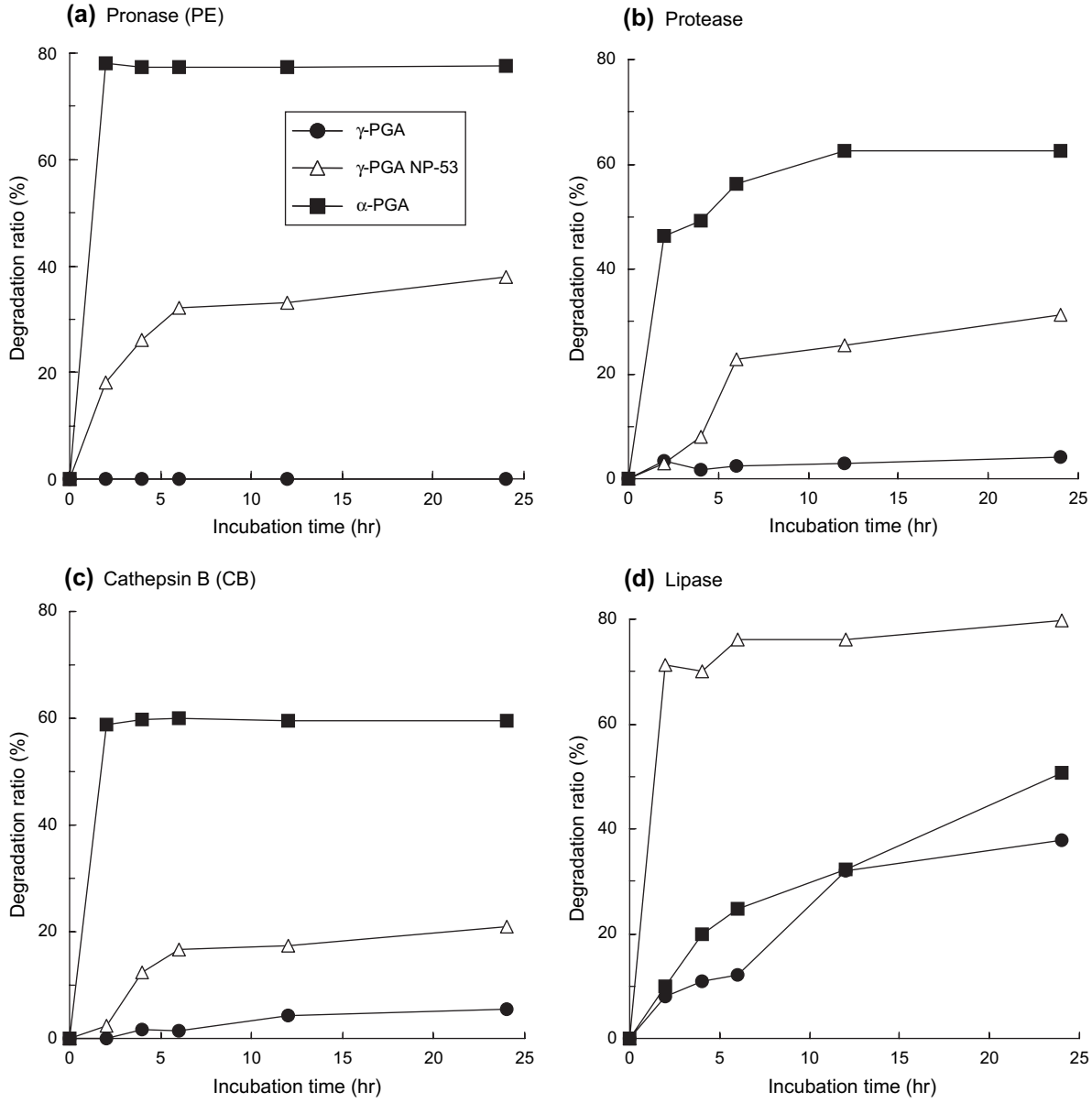

Fig. 16. Enzymatic degradation of γ-PGA, γ-hPGA nanoparticles (γ-PGA-NP-53) and α-PGA by Pronase E (PE) (a), protease from *A. sojae* (protease) (b), cathepsin B (CB) (c), and lipase (d) for different incubation periods at 37 °C. The degradation ratio was calculated as: $[(M_{n_0} - M_{n_t})/M_{n_0}] \times 100$. Data from Ref. [115].

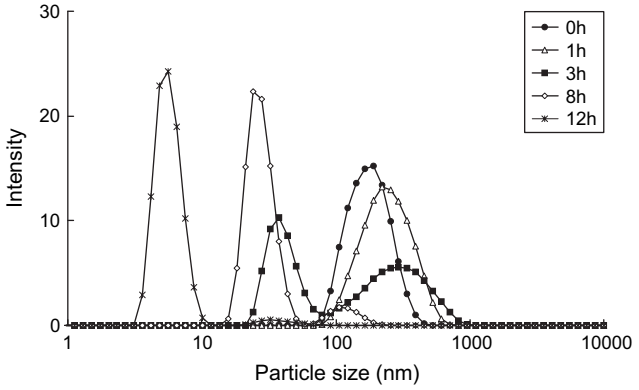

Fig. 17. Changes in the size of γ-hPGA nanoparticles (γ-PGA-NP-53) as a function of the degradation time with Pronase E (PE). The size distribution of the γ-hPGA nanoparticles was measured in PBS by DLS. Data from Ref. [115].

the α-carboxylate side chains of γ-PGA and L-PAE occurred using PE, protease, CB, and lipase.

Fig. 17 shows the change in the particle size of γ-PGA-NP-53 as the degradation progressed with PE [115]. The size of the nanoparticles increased slightly from 190 to 257 nm during the first 1 h, and then gradually decreased with time. These results suggest that the enzymatic cleavage of L-PAE may lead to a lighter packing density of the core of the nanoparticles. Therefore, the increase in particle size at the initial degradation may be attributed to an increase in the swelling capacity due to the cleavage of L-PAE in the core of the nanoparticles. On the other hand, the hydrophobic interactions of L-PAE attached to γ-PGA were significantly reduced upon increasing the degradation time, since it is not sufficient to form any nanoparticles. Therefore, the decrease in the particle size with further degradation probably occurs upon the dissociation of γ-PGA-*graft*-L-PAE from the nanoparticles, or via the aggregation of γ-PGA-*graft*-L-PAE detached from the nanoparticles. During the degradation process, the size of the γ-PGA nanoparticles changed significantly. It has also been reported that the hydrolytic degradation of amphiphilic block copolymer micelles affects their particle size and morphologies [132].

6. Preparation and characterization of protein-loaded γ-hPGA nanoparticles

Biodegradable polymeric nanoparticles are generally formulated using the emulsion solvent evaporation method. Surfactants are often used to stabilize the nanoparticles in aqueous solution in order to prevent the aggregation and/or precipitation of water insoluble polymers, such as PLA and PCL [133]. However, adequate removal of the surfactant remains a problem and surfactant molecules are sometimes harmful in biomedical applications. Moreover, the water-in-oil-in-water (w/o/w) double emulsion process is typically used to load proteins into nanoparticles. It has a disadvantage in that these solvents have a denaturing effect on the proteins [134,135]. In addition, during the degradation process, a low pH is generated inside the biodegradable nanoparticles. In this method, the entrapped protein may be denatured, aggregated and chemically degraded [136,137]. Therefore, a novel type of nanoparticle needs to be developed.

6.1. Encapsulation of proteins into γ-hPGA nanoparticles

Protein-encapsulated γ-hPGA nanoparticles were prepared in order to study their potential applications as protein carriers. To prepare the protein-encapsulated γ-hPGA nanoparticles, 0.25–4 mg of protein (thyroglobulin, catalase, Con A, bovine serum albumin (BSA), ovalbumin (OVA), peroxidase, β-lactoglobulin, myoglobin, lysozyme, α-lactalbumin, and cytochrome c) was dissolved in 1 ml of saline and 1 ml of γ-PGA-*graft*-L-PAE-53 (10 mg/ml in DMSO) was added to the protein solution. The resulting solution was centrifuged and repeatedly rinsed. The protein loading content was then measured by Lowry method [113,114].

The encapsulation of proteins of various molecular weights and isoelectric points into the nanoparticles was successfully achieved. The results of the encapsulation of protein into the nanoparticles are summarized in Table 3 [114]. All proteins used in this experiment were successfully encapsulated into the nanoparticles. The encapsulation efficiency was found to be in the range of 30–60% for most samples. The amount of protein encapsulated into the nanoparticles was increased upon increasing the initial feeding amount of protein (Fig. 18) [114]. For all samples tested, it was observed that the encapsulation efficiency for a given protein was not markedly influenced by the physical properties of that protein. Wang et al. reported that nanoparticles prepared from amphiphilic poly-L-lysine were able to encapsulate hydrophilic dextran [93].

From the DLS measurements, the mean diameter of the unloaded γ-hPGA nanoparticles was 180 nm with a monodispersed size distribution. The particle size of the nanoparticles was increased when various proteins were encapsulated (Table 3). These results might be due to an increase in the swelling capacity of the nanoparticles due to the hydrophilic properties of the protein [113]. Na et al. reported that the introduction of vitamin H into hydrophobically modified pullulan, pullulan acetate, enhanced the formation of swelling hydrogel nanoparticles due to the hydrophilicity of vitamin H [138]. In the preparation of lysozyme-encapsulated nanoparticles, a large amount of aggregation was found. This result can be attributed to the strong electrostatic interaction between lysozyme and the nanoparticles at the time of particle formation. These interactions may disturb the stable formation of inner cores and thus they could not form monodispersed nanoparticles.

6.2. Characterization of protein-encapsulated γ-hPGA nanoparticles

To study the protein release behavior, OVA-encapsulated γ-hPGA nanoparticles were suspended in buffers of varying pH values and the OVA release was then determined *in vitro*.

Table 3
Entrapment efficiency, particle size and zeta potential of protein-encapsulated γ-hPGA nanoparticles

Protein	Molecular weight × 10^3 (M_w)	Isoelectric point (p*I*)	Entrapment efficiency[a] (wt.%)	Loading content[b] (μg/NP 1 mg)	Particle size[c] (nm)	Polydispersity	Zeta potential[c] (mV)
Thyroglobulin	670	4.5	52.4	104.9	281	0.29	−20.5 ± 2.6
Catalase	232	5.5	60.0	120.1	320	0.26	−20.9 ± 3.6
Concanavalin A	104	5.0	51.9	103.8	340	0.26	−20.0 ± 5.1
Bovine serum albumin	69	4.9	58.5	116.9	289	0.27	−20.9 ± 5.3
Ovalbumin	45	4.6	45.0	90.0	256	0.29	−21.6 ± 2.4
Peroxidase	44	7.5	25.3	50.5	202	0.16	−23.9 ± 4.4
β-Lactoglobulin	18	5.2	38.6	77.2	233	0.21	−23.4 ± 1.9
Myoglobin	17.5	7.3	44.6	89.2	212	0.22	−24.0 ± 4.4
Lysozyme	14.5	11.0	31.3	62.6	>3000	1.00	−15.1 ± 7.0
α-Lactalbumin	14.0	5.0	28.2	56.3	198	0.22	−24.8 ± 4.1
Cytochrome *c*	12.5	10.2	43.8	87.6	353	0.26	−17.0 ± 6.4
γ-hPGA nanoparticles					180	0.12	−23.8 ± 2.4

Data from Ref. [114].
[a] γ-PGA-*graft*-L-PAE-53 copolymers and each proteins were mixed to a final concentration of 5 mg/ml and 1 mg/ml. The entrapment efficiency was measured as (total encapsulated protein weight/initial feeding amount of protein weight) × 100.
[b] The amount of protein loading into γ-hPGA nanoparticles was calculated by loaded protein weight (μg)/nanoparticles (NP) weight (1 mg).
[c] Particle size and zeta potential of γ-hPGA nanoparticles were measured in PBS by a Zetasizer nano ZS.

The release of OVA from nanoparticles with an OVA content of 43 μg/NP 1 mg was performed at 37 °C. OVA encapsulated into the nanoparticles was not released (less than 10%) over the pH range of 4–8, even after 10 days (data not shown) [113]. These results suggest that the γ-PGA backbone composed of γ-linked glutamic acid and the amide bond between the α-carboxylate side chains of γ-PGA and L-PAE is not degraded under these experimental conditions. It is expected that protein-encapsulated γ-hPGA nanoparticles can release protein in the cell or *in vivo* upon enzymatic digestion.

The absence or slow release of OVA from the nanoparticles can be explained as a consequence of the interaction between OVA and γ-PGA-*graft*-L-PAE. In the case of peptide encapsulation with different hydrophobicities, the peptide with the higher hydrophobicity showed a higher encapsulation efficiency (data not shown). Therefore, the interaction between OVA and the nanoparticles may be due to the hydrophobic interactions between the hydrophobic regions of OVA and the hydrophobic L-PAE groups [114]. The inner structures of the nanoparticles are likely to retain the flexibility of the protein encapsulated into the nanoparticles. In the case of nanoparticles prepared from amphiphilic diblock PLA–PEG copolymer nanoparticles, the hydrophobic interactions between the hydrophobic regions of the protein and the hydrophobic PLA blocks were observed [139].

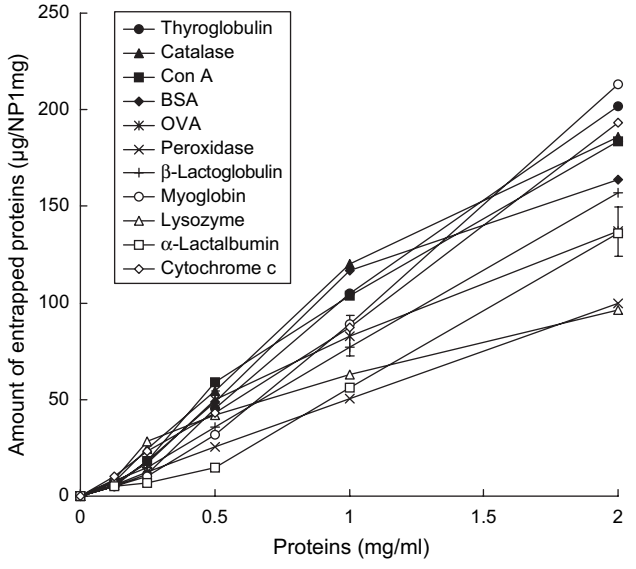

Fig. 18. Effects of the protein concentration on the amount of protein encapsulated into γ-hPGA nanoparticles (γ-PGA-NP-53). γ-PGA-*graft*-L-PAE (in DMSO) and protein solutions were mixed to a final copolymer concentration of 5 mg/ml. The amount of protein encapsulated into the nanoparticles was calculated as the loaded protein weight (μg)/nanoparticle weight (1 mg). Data from Ref. [114].

Since freeze drying is a convenient technique for nanoparticle storage, the effects of freeze drying on the size of the γ-hPGA nanoparticles and the OVA-encapsulated nanoparticles were studied. After freeze drying, these nanoparticles were easily re-dispersed in water, and their particle size showed no change as compared to before freeze drying (data not shown). The total amount of OVA leaked from the lyophilized nanoparticles was less than 5% of the total OVA loaded. These results indicate that the γ-PGA nanoparticles and OVA-encapsulated nanoparticles have high stability for the freeze-drying process [113].

6.3. Surface immobilization of protein onto γ-hPGA nanoparticles

Protein-loaded γ-PGA nanoparticles could be prepared by the surface immobilization method. Various proteins were covalently immobilized onto the nanoparticles by amide bonds between the carboxyl groups on the surface of the γ-hPGA nanoparticles and the protein amide groups. The results of the entrapment of various proteins onto the nanoparticles are shown in Fig. 19 [114]. The amount of protein immobilized onto the nanoparticles showed different trends at various molecular weights and isoelectric points of the protein.

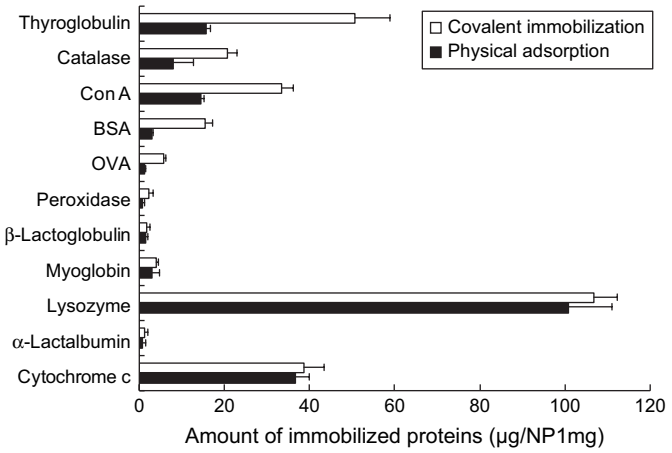

Fig. 19. Immobilization and adsorption of various proteins onto the surface of γ-hPGA nanoparticles (γ-PGA-NP-53). γ-hPGA nanoparticles treated (covalent immobilization) or untreated (physical adsorption) with 500 μg/ml of WSC, nanoparticles and each protein solution were mixed, to final concentrations of 5 mg/ml and 1.75 mg/ml, respectively. The results are presented as means ± SD values ($n = 3$). Data from Ref. [114].

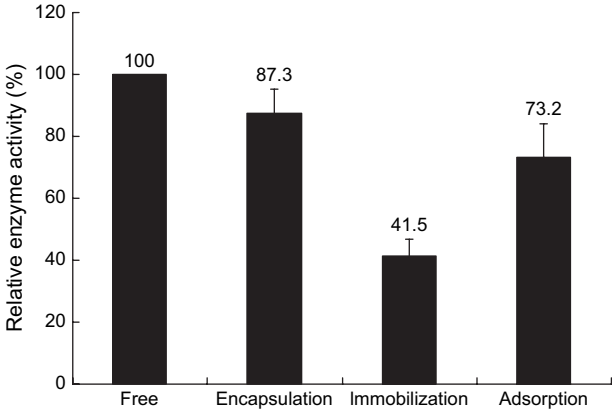

Fig. 20. Effects of the conjugation method on the activity of catalase. The catalase activities of free catalase (free), catalase-encapsulated (encapsulation), catalase-immobilized (immobilization), and catalase-adsorbed (adsorption) γ-hPGA nanoparticles (γ-PGA-NP-53) were determined spectrophotometrically by the direct measurement of the decrease in the absorbance of hydrogen peroxide (20 mM) at 240 nm. The results are presented as means ± SD values ($n = 3$). Data from Ref. [114].

At higher molecular weights, the amount of protein covalently immobilized was larger at a lower molecular weight. On the other hand, lysozyme and cytochrome *c* were adsorbed with high yields. Positively charged proteins could be adsorbed onto negatively charged nanoparticles by electrostatic interactions. It is known that protein loading into micro/nanoparticles is influenced by both electrostatic interactions and other mechanisms such as hydrophobic interactions and structural accommodation of the polymer and biomolecule [140]. Except for lysozyme, the entrapment efficiency onto the surface of nanoparticles using WSC was only about 1–10%. These results demonstrate that the entrapment efficiency for a given protein is significantly dependent on the conjugation method.

The surface area of nanoparticles per milligram was 200 cm^2 for 200 nm-sized nanoparticles. In the case of OVA surface immobilization, the theoretical amount of OVA immobilized onto the surface was about 80 μg/NP 1 mg at maximum. On the other hand, the amount of OVA encapsulated into the nanoparticles was about 150 μg/NP 1 mg (initial OVA conc. 2 mg/ml). The loading capacity of OVA into the nanoparticles was higher than the theoretical amount of OVA immobilized onto the surface [113]. Thus, the interior space of the nanoparticles has great potential to load proteins. When compared with the amount of protein loading, the encapsulation method appeared to be more effective than the immobilization method.

6.4. Effect of the conjugation method on catalase activity

The effect of the conjugation method on the enzymatic activity of catalase-entrapped γ-hPGA nanoparticles was also evaluated using H_2O_2. Catalase-entrapped nanoparticles were prepared by the encapsulation (48 μg/NP 1 mg), covalent immobilization (27 μg/NP 1 mg), and physical adsorption (13 μg/NP 1 mg) methods. Fig. 20 shows the activity of the catalase-entrapped in/onto the nanoparticles [114]. The catalase activity was significantly affected by the conjugation method. For encapsulation, the catalase activity was higher than that of the immobilization and adsorption methods. The catalase covalently immobilized onto the nanoparticles showed the lowest activity in these conjugation methods. Based on these results, it is likely that the interactions between the proteins and nanoparticles in the protein-encapsulated nanoparticles were weaker than those of the immobilization and adsorption methods, and protein flexibility was not impaired significantly by its encapsulation. The stability of the protein encapsulated into the nanoparticles may be attributed to the preparation method of protein-encapsulated nanoparticles.

In this study, protein-encapsulated nanoparticles were prepared by a precipitation and centrifugal washing method. In the case of protein-encapsulated nanoparticles prepared by the self-assembly of γ-PGA-*graft*-L-PAE, the encapsulated protein may be more stable than via the emulsion method. Proteins encapsulated into the γ-hPGA nanoparticles appear to be adequate in terms of the preservation of the protein structure. Protein stability in nanoparticles is considered to play a significant role in the induction of adequate immune responses for vaccines [141,142]. In this experiment, encapsulation was the optimal method for the conjugation of proteins and nanoparticles. In fact, immunization of mice with protein antigen-encapsulated γ-hPGA nanoparticles strongly induced antigen-specific humoral and cellular immunity [143]. This system provides a novel delivery tool and an efficient antigen delivery system in the development of protein-based vaccines.

7. Conclusions

Monodispersed polymeric nanoparticles, which consist of a hydrophobic core and a hydrophilic corona on their surfaces, were prepared by the free radical dispersion copolymerization

of hydrophobic monomers and hydrophilic macromonomers in a polar solvent. Core-corona type nanoparticles could be widely utilized for various technological and biomedical applications, because of their possible variety of chemical structures. These nanoparticles were utilized as oral drug carriers for peptide drugs physically adsorbed onto the nanoparticle surfaces. Moreover, lectin-immobilized nanoparticles could efficiently capture HIV-1 particles and have great potential as a prophylactic vaccine against HIV-1 infection. Based on these studies, we attempted to develop novel biodegradable nanoparticles composed of γ-hPGA. Protein-entrapped γ-hPGA nanoparticles were prepared in order to study their potential applications as protein carriers. It is expected that biodegradable γ-hPGA nanoparticles can encapsulate and immobilize proteins, peptides, plasmid DNA, and drugs. These multifunctional nanoparticles have great potential as carriers for biomolecules. These characteristics strongly suggest that γ-PGA nanoparticles can be developed as useful vaccine carriers for modulated biodistribution, as well as site and/or cell-specific drug delivery systems. Nanoparticles prepared by the self-organization of polymers consisting of hydrophobic and hydrophilic segments show promise as drug delivery systems as a result of their controlled- and sustained-release properties, subcellular size, and biocompatibility with tissue and cells.

Acknowledgments

This work was supported by Core Research for Evolutional Science and Technology (CREST) from the Japan Science and Technology Agency (JST).

References

[1] Soppimath KS, Aminabhavi TM, Kulkarni AR, Rudzinski WE. J Controlled Release 2001;70:1–20.
[2] Brigger I, Dubernet C, Couvreur P. Adv Drug Deliv Rev 2002;54:631–51.
[3] Pinto Reis C, Neufeld RJ, Ribeiro AJ, Veiga F. Nanomedicine 2006;2:8–21.
[4] Hans ML, Lowman AM. Curr Opin Solid State Mater Sci 2002;6:319–27.
[5] Panyam J, Labhasetwar V. Adv Drug Deliv Rev 2003;55:329–47.
[6] Allen TM, Cullis PR. Science 2004;303:1818–22.
[7] Koping-Hoggard M, Sanchez A, Alonso MJ. Expert Rev Vaccines 2005;4:185–96.
[8] Yih TC, AI-Fandi M. J Cell Biochem 2006;97:1184–90.
[9] Zhang L, Eisenberg A. J Am Chem Soc 1996;118:3168–81.
[10] Liu XM, Pramoda KP, Yang YY, Chow SY, He C. Biomaterials 2004;25(26):19–28.
[11] Jaturanpinyo M, Harada A, Yuan X, Kataoka K. Bioconjugate Chem 2004;15:344–8.
[12] Akiyoshi K, Kobayashi S, Shichibe S, Mix D, Baudys M, Kim SW, et al. J Controlled Release 1998;54:313–20.
[13] Jung SW, Jeong YI, Kim SH. Int J Pharm 2003;254:109–21.
[14] Na K, Park KH, Kim SW, Bae YH. J Controlled Release 2000;69:225–36.
[15] Gref R, Rodrigues J, Couvreur P. Macromolecules 2002;35:9861–7.
[16] Leonard M, Boisseson MRD, Hubert P, Dalenccon F, Dellacherie E. J Controlled Release 2004;98:395–405.
[17] Park JH, Kwona S, Nam JO, Park RW, Chung H, Seo SB, et al. J Controlled Release 2004;95:579–88.
[18] Akiyoshi K, Deguchi S, Moriguchi N, Yamaguchi S, Sunamoto J. Macromolecules 1993;26:3062–8.
[19] Akashi M, Kirikihira I, Miyauchi N. Angew Makromol Chem 1985;132:81–9.
[20] Akashi M, Yanagi T, Yashima E, Miyauchi N. J Polym Sci Part A Polym Chem 1989;27:3521–30.
[21] Matsusaki M, Hiwatari K, Higashi M, Kaneko T, Akashi M. Chem Lett 2004;33:398–9.
[22] Kaneko T, Higashi M, Matsusaki M, Akagi T, Akashi M. Chem Mater 2005;17:2484–6.
[23] Matsusaki M, Fuchida T, Kaneko T, Akashi M. Biomacromolecules 2005;6:2374–9.
[24] Behan N, Birkinsha C, Clarke N. Biomaterials 2001;22:1335–44.
[25] Reis CP, Neufeld RJ, Vilela S, Ribeiro AJ, Veiga F. J Microencapsul 2006;23:245–57.
[26] Zhang L, Eisenberg A. Science 1995;268:1728–31.
[27] Zhang W, Shi L, An Y, Shen X, Guo Y, Gao L, et al. Langmuir 2003;19:6026–31.
[28] Wang W, Qu X, Gray AI, Tetley L, Uchegbu IF. Macromolecules 2004;37:9114–22.
[29] Iijima M, Nagasaki Y, Okada T, Kato M, Kataoka K. Macromolecules 1999;32:1140–6.
[30] Allen C, Han J, Yu Y, Maysinger D, Eisenberg A. J Controlled Release 2000;63:275–86.
[31] Akashi M, Chao D, Yashima E, Miyauchi N. J Appl Polym Sci 1990;39:2027–30.
[32] Capek I, Riza M, Akashi M. Polym J 1992;24:959–70.
[33] Capek I, Riza M, Akashi M. Makromol Chem 1992;193:2843–60.
[34] Capek I, Akashi M. J Macromol Sci Rev Macromol Chem Phys 1993;33:369–436.
[35] Riza M, Capek I, Kishida A, Akashi M. Angew Makromol Chem 1993;206:69–75.
[36] Riza M, Tokura S, Kishida A, Akashi M. New Polym Mater 1994;4:189–98.
[37] Riza M, Tokura S, Iwasaki M, Yashima E, Kishida A, Akash M. J Polym Sci Part A Polym Chem 1995;33:1219–25.
[38] Capek I, Riza M, Akashi M. Eur Polym J 1995;31:895–902.
[39] Chen MQ, Kishida A, Akashi M. J Polym Sci Part A Polym Chem 1996;34:2213–20.
[40] Wu C, Akashi M, Chen MQ. Macromolecules 1997;30:2187–9.
[41] Serizawa T, Chen MQ, Akashi M. Langmuir 1998;14:1278–80.
[42] Serizawa T, Chen MQ, Akashi M. J Polym Sci Part A Polym Chem 1998;36:2581–7.
[43] Chen MQ, Serizawa T, Akashi M. Polym Adv Technol 1999;10:120–6.
[44] Chen MQ, Serizawa T, Kishida A, Akashi M. J Polym Sci Part A Polym Chem 1999;37:2155–66.
[45] Chen MQ, Kishida A, Serizawa T, Akashi M. J Polym Sci Part A Polym Chem 2000;38:1811–7.
[46] Serizawa T, Takehara S, Akashi M. Macromolecules 2000;33:1759–64.
[47] Hiwatari K, Serizawa T, Akashi M. Polym J 2001;33:424–8.
[48] Serizawa T, Yanagisono Y, Ueno M, Akashi M. Polym J 2005;37:39–42.
[49] Takeuchi S, Okie M, Kowitz C, Shimasaki C, Hasegawa K, Kitano H. Makromol Chem 1993;194:551–8.
[50] Kawaguchi H, Winnik MA, Ito K. Macromolecules 1995;28:1159–66.
[51] Ishizu K, Tahara N. Polymer 1996;37:1729–34.
[52] Serizawa T, Taniguchi K, Akashi M. Colloids Surf 2000;169:95–105.
[53] Akashi M, Niikawa T, Serizawa T, Hayakawa T, Baba M. Bioconjugate Chem 1998;9:50–3.
[54] Sakuma S, Hayashi M, Akashi M. Adv Drug Deliv Rev 2001;47:21–37.
[55] Serizawa T, Uchida T, Akashi M. J Biomater Sci Polym Ed 1999;10:391–401.
[56] Serizawa T, Yasunaga S, Akashi M. Biomacromolecules 2001;2:469–75.
[57] Chen CW, Chen MQ, Serizawa T, Akashi M. Chem Commun 1998;7:831–2.

[58] Chen CW, Chen MQ, Serizawa T, Akashi M. Adv Mater 1998;10: 1122–6.
[59] Chen CW, Serizawa T, Akashi M. Langmuir 1999;15:7998–8006.
[60] Chen CW, Serizawa T, Akashi M. Chem Mater 1999;11:1381–9.
[61] Chen CW, Arai K, Yamamoto K, Serizawa T, Akashi M. Macromol Chem Phys 2000;201:2811–9.
[62] Chen CW, Serizawa T, Akashi M. Chem Mater 2002;14:2232–9.
[63] Allemann E, Leroux J, Gurny R. Adv Drug Deliv Rev 1998;34:171–89.
[64] Takeuchi H, Yamamoto H, Kawashima Y. Adv Drug Deliv Rev 2001;47:39–54.
[65] Prego C, Garcia M, Torres D, Alonso MJ. J Controlled Release 2005; 101:151–62.
[66] Lee VHL, Yamamoto A. Adv Drug Deliv Rev 1990;4:171–207.
[67] Sakuma S, Suzuki N, Kikuchi H, Hiwatari K, Arikawa K, Kishida A, et al. Int J Pharm 1997;149:93–106.
[68] Sakuma S, Suzuki N, Kikuchi H, Hiwatari K, Arikawa K, Kishida A, et al. Int J Pharm 1997;158:69–78.
[69] Sakuma S, Suzuki N, Sudo R, Hiwatari K, Kishida A, Akashi M. Int J Pharm 2002;239:185–95.
[70] Takeuchi H, Yamamoto H, Niwa T, Hino T, Kawashima Y. Pharm Res 1996;13:896–901.
[71] Sakuma S, Sudo R, Suzuki N, Kikuchi H, Hiwatari K, Akashi M, et al. Int J Pharm 1999;177:161–72.
[72] Sakuma S, Ishida Y, Sudo R, Suzuki N, Kikuchi H, Hiwatari K, et al. Int J Pharm 1997;159:181–9.
[73] Sakuma S, Sudo R, Suzuki N, Kikuchi H, Akashi M, Ishida Y, et al. J Controlled Release 2002;81:281–90.
[74] Kubitschko S, Spinke J, Bruckner T, Pohl S, Oranth N. Anal Biochem 1997;253:112–22.
[75] Shen S, Tu S. Biotechnol Appl Biochem 1999;29:185–9.
[76] Akagi T, Ueno M, Hiraishi K, Baba M, Akashi M. J Controlled Release 2005;109:49–61.
[77] Gattegno L, Ramdani A, Jouault T, Saffar L, Gluckman JC. AIDS Res Hum Retroviruses 1992;8:27–37.
[78] Lifson J, Coutre S, Huang E, Engleman E. J Exp Med 1986;164:2101–6.
[79] Hayakawa T, Kawamura M, Okamoto M, Baba M, Niikawa T, Takehara S, et al. J Med Virol 1998;56:327–31.
[80] Cetinus SA, Oztop HN. Enzyme Microb Technol 2003;32:889–94.
[81] Kang K, Kan C, Yeung A, Liu D. Macromol Biosci 2005;5:344–51.
[82] Zhao Z, Leong KW. J Pharm Sci 1996;85:261–70.
[83] Singh M, O'Hagan DT. Pharm Res 2002;19:715–28.
[84] O'Hagan DT, Lavelle E. AIDS 2002;16:115–24.
[85] Wang X, Uto T, Sato K, Ide K, Akagi T, Okamoto M, et al. Immunol Lett 2005;98:123–30.
[86] Matsusaki M, Larsson K, Akagi T, Lindstedt M, Akashi M, Borrebaeck CA. Nano Lett 2005;5:2168–73.
[87] Kawamura M, Naito T, Ueno M, Akagi T, Hiraishi K, Takai I, et al. J Med Virol 2002;66:291–8.
[88] Akagi T, Kawamura M, Ueno M, Hiraishi K, Adachi M, Serizawa T, et al. J Med Virol 2003;69:163–72.
[89] Kawamura M, Wang X, Uto T, Sato K, Ueno M, Akagi T, et al. J Med Virol 2005;76:7–15.
[90] Miyake A, Akagi T, Enose Y, Ueno M, Kawamura M, Horiuchi R, et al. J Med Virol 2004;73:368–77.
[91] Holowka EP, Pochan DJ, Deming TJ. J Am Chem Soc 2005;127: 12423–8.
[92] Arimura H, Ohya Y, Ouchi T. Biomacromolecules 2005;6:720–5.
[93] Wang W, Tetley L, Uchegbu IF. Langmuir 2000;16:7859–66.
[94] Akiyoshi K, Ueminami A, Kurumada S, Nomura Y. Macromolecules 2000;33:6752–6.
[95] Holowka EP, Sun VZ, Kamei DT, Deming TJ. Nat Mater 2007;6:52–7.
[96] Jeong JH, Kang HS, Yang SR, Kim JD. Polymer 2003;44:583–91.
[97] Liang HF, Chen SC, Chen MC, Lee PW, Chen CT, Sung HW. Bioconjugate Chem 2006;17:291–9.
[98] Liang HF, Yang TF, Huang CT, Chen MC, Sung HW. J Controlled Release 2005;105:213–25.
[99] Liang HF, Chen CT, Chen SC, Kulkarni AR, Chiu YL, Chen MC, et al. Biomaterials 2006;27:2051–9.
[100] Kataoka K, Matsumoto T, Yokoyama M, Okano T, Sakurai Y, Fukushima S, et al. J Controlled Release 2000;64:143–53.
[101] Lin J, Zhang S, Chen T, Lin S, Jin H. Int J Pharm 2007;336:49–57.
[102] Lee ES, Shin HJ, Na K, Bae YH. J Controlled Release 2003;90: 363–74.
[103] Kubota H, Matsunobu T, Uotani K, Takebe H, Satoh A, Tanaka T, et al. Biosci Biotechnol Biochem 1993;57:1212–3.
[104] Oppermann FB, Fickaitz S, Steinbuchel A. Polym Degrad Stab 1998;59:337–44.
[105] Obst M, Steinbuchel A. Biomacromolecules 2004;5:1166–76.
[106] Kishida A, Murakami K, Goto H, Akashi M, Kubota H, Endo T. J Bioact Compat Polym 1998;13:270–8.
[107] Matsusaki M, Serizawa T, Kishida A, Endo T, Akashi M. Bioconjugate Chem 2002;13:23–8.
[108] Shimokuri T, Kaneko T, Serizawa T, Akashi M. Macromol Biosci 2004;4:407–11.
[109] Wang W, McConaghy AM, Tetley L, Uchegbu IF. Langmuir 2001;17: 631–6.
[110] Guan H, Xie Z, Zhang P, Deng C, Chen X, Jing X. Biomacromolecules 2005;6:1954–60.
[111] Akagi T, Higashi M, Kaneko T, Kida T, Akashi M. Macromol Biosci 2005;5:598–602.
[112] Duval-Terrie C, Huguet J, Muller G. Colloids Surf A 2003;220:105–15.
[113] Akagi T, Kaneko T, Kida T, Akashi M. J Controlled Release 2005;108:226–36.
[114] Akagi T, Kaneko T, Kida T, Akashi M. J Biomater Sci Polym Ed 2006;17:875–92.
[115] Akagi T, Higashi M, Kaneko T, Kida T, Akashi M. Biomacromolecules 2006;7:297–303.
[116] O'Hagan DT, Jeffery H, Davis SS. Int J Pharm 1994;103:37–45.
[117] Li X, Deng X, Yuan M, Xiong C, Huang Z, Zhang Y, et al. J Appl Polym Sci 2000;78:140–8.
[118] Liggins RT, Burt HM. Int J Pharm 2001;222:19–33.
[119] Zhang Y, Zhuo R. Biomaterials 2005;26:6736–42.
[120] Nie T, Zhao Y, Xie Z, Wu C. Macromolecules 2003;36:8825–9.
[121] Xiong XY, Gan LH, Tam KC. Macromolecules 2004;37:3425–30.
[122] Hayashi T, Nakanishi E, Iizuka Y, Oya M, Iwatsuki M. Eur Polym J 1995;31:453–8.
[123] Chiu HC, Kopeckova P, Deshmane SS, Kopecek J. J Biomed Mater Res 1997;34:381–92.
[124] Rypacek F. Polym Degrad Stab 1998;59:345–51.
[125] Li C. Adv Drug Deliv Rev 2002;54:695–713.
[126] Fan K, Gonzales D, Sevoian M. J Environ Polym Degrad 1996;4: 253–60.
[127] Goto A, Kunioka M. Biosci Biotechnol Biochem 1992;56:1031–5.
[128] Martinez Barbosa ME, Cammas S, Appel M, Ponchel G. Biomacromolecules 2004;5:137–43.
[129] Kubota H, Nanbu Y, Endo T. J Polym Sci Part A Polym Chem 1996;34: 1347–51.
[130] Abe K, Ito Y, Ohmachi T, Asada Y. Biosci Biotechnol Biochem 1997;61:1621–5.
[131] Weber J. J Biol Chem 1990;265:9664–8.
[132] Hu Y, Zhang L, Cao Y, Ge H, Jiang X, Yang C. Biomacromolecules 2004;5:1756–62.
[133] Lemoine D, Francois C, Kedzierewicz F, Preat V, Hoffman M, Maincent P. Biomaterials 1996;17:2191–7.
[134] Sah H. J Controlled Release 1999;58:143–51.
[135] van de Weert M, Hennink WE, Jiskoot W. Pharm Res 2000;17: 1159–67.
[136] Park TG, Lu W, Crotts G. J Controlled Release 1995;332:211–22.
[137] Panyam J, Dali MM, Sahoo SK, Ma W, Chakravarthi SS, Amidon GL, et al. J Controlled Release 2003;92:173–87.
[138] Na K, Lee TB, Park KH, Shin EK, Lee YB, Choi HK. Eur J Pharm Sci 2003;18:165–73.
[139] Quellec P, Gref R, Perrin L, Dellacherie E, Sommer F, Verbavatz JM, et al. J Biomed Mater Res 1998;42:45–54.
[140] Singh M, Chesko J, Kazzaz J, Ugozzoli M, Kan E, Srivastava I, et al. Pharm Res 2004;212:2148–52.

[141] Regine A, Ying M, Pal J, Bruno G, Giampietro G. Pharm Res 1998;15:1111–6.
[142] Lavelle EC, Yeh MK, Coombes AG, Davis SS. Vaccine 1999;17: 512–29.
[143] Akagi T, Wang X, Uto T, Baba M, Akashi M. Biomaterials 2007;28:3427–36.

Takami Akagi was born in 1973. He received his B.S. (1996) and M.S. (1998) degrees in Applied Chemistry and Chemical Engineering from Kagoshima University, and Ph.D. degree (2005) in Engineering from Osaka University, Japan. He joined the Department of Pharmacological Science at Japan Immunoresearch Laboratories (JIMRO) Co., Ltd. in 1998–2003. Then he was moved to the Graduate School of Engineering, Osaka University as a Japan Science and Technology Agency (JST) researcher in 2003. Currently he is engaged in the JST project of Core Research for Evolutional Science and Technology (CREST). This project is aimed at the development of anti-retroviral vaccine using polymeric nanoparticles. His research interests include the development of self-assembled nanoparticles consisting of amphiphilic biodegradable polymers capable of regulation of immuno responses.

Masanori Baba is the Professor of Antiviral Chemotherapy at the Graduate School of Medical and Dental Sciences, Kagoshima University, Japan. He received his M.D. degree in 1980 and Ph.D. degree in Microbiology from Fukushima Medical College, Japan in 1985. After a postdoctoral fellowship at the Rega Institute, Katholieke Universiteit Leuven, Belgium, he joined the Department of Bacteriology, Fukushima Medical College in 1989. In 1996, he became a Professor at the Center for Chronic Viral Diseases in Kagoshima University. Dr. Baba is a member of the Board of Directors of the International Society of Antiviral Research (ISAR) and the Japanese Association of Antiviral Therapy (JAAT). He has been a member of the Editorial Board for *Antimicrobial Agents and Chemotherapy* and *Antiviral Research* for more than 10 years and as an editor for *Antiviral Chemistry and Chemotherapy.* He is an ISI Highly Cited researcher in the Microbiology category since 2002.

Mitsuru Akashi received his Ph.D. degree in Engineering from Osaka University in 1978. He was a postdoc at NIH, Gerontology Research Center, USA, in 1978–1979, and Department of Chemical Engineering, University of Waterloo, Canada, in 1979–1980. He joined the Department of Applied Chemistry and Chemical Engineering, Faculty of Engineering, Kagoshima University as an assistant professor in 1981. He was promoted to associate professor in 1984 and a full professor in 1989. From 2003, he is a full professor for the Department of Applied Chemistry, Graduate School of Engineering, Osaka University. He received the Award of the Society of Polymer Science, Japan (1999) and the Award of Japanese Society for Biomaterials (2004). His research interests cover design and synthesis of functional polymers and preparation of novel biomaterials, including synthesis of biodegradable nanoparticles and gels.